WSRC-TR-96-0080
Rev 0
April 1996

Ground Penetrating Radar and Direct Current Resistivity Evaluation of the Desiccation Test Cap, Savannah River Site (U)

Westinghouse Savannah River Company
Savannah River Site
Aiken, SC 29808

SAVANNAH RIVER SITE

Prepared for the U.S. Department of Energy under contract no. DE-AC09-89SR18035

WSRC-TR-96-0080
Rev 0

Ground Penetrating Radar and Direct Current Resistivity Evaluation of the Desiccation Test Cap, Savannah River Site(U)

D. E. Wyatt
R. J. Cumbest
Site Geotechnical Services

Prepared for the U.S. Department of Energy under contract no. DE-AC09-89SR18035

Contents

Page

LIST OF FIGURES

INTRODUCTION

The Savannah River Site (SRS) has a variety of waste units that may be temporarily or permanently stabilized by closure using an impermeable cover to prevent groundwater infiltration. The placement of an engineered kaolin clay layer over a waste unit is an accepted and economical technique for providing an impermeable cover but the long term stability and integrity of the clay in non-arid conditions is unknown. Numerous factors may affect clay and cap integrity, including desiccation, erosion, bioturbation, physical damage and structural failure.

A simulated kaolin cap has been constructed at the SRS adjacent to the Burial Ground Complex (Figure 1). The cap is designed to evaluate the effects of desiccation on clay integrity, therefore half of the cap is covered with native soil to prevent drying, while the remainder of the cap is exposed. Infiltrometers are installed within a portion of the covered cap and the remainder of the area is available for additional studies.

Measurements of the continuing impermeability of a clay cap are difficult because intrusive techniques may locally compromise the structure. Point measurements made to evaluate clay integrity, such as those from grid sampling or coring and made through a soil cover, may miss cracks, joints or fissures, and may not allow for mapping of the lateral extent of elongate features. Because of these problems, a non-invasive technique is needed to map clay integrity, below a soil or vegetation cover, which is capable of moderate to rapid investigation speeds.

Two non-intrusive geophysical techniques, direct current resistivity and ground penetrating radar (GPR), have been successful at the SRS in geologically mapping shallow subsurface clay layers. The applicability of each technique in detecting the clay layer in the desiccation test cap and associated anomalies was investigated.

THEORY

Surface resistivity profiling is a well known and understood geophysical tool using an induced direct electrical current to measure the apparent resistivity of subsurface sediments. In the Wenner Array method, current and potential electrodes are equally spaced with the potential electrodes in the center of the array and the current electrodes on the outside of the array. A reversing DC current is applied to the outer electrodes which sets up an electric field in the subsurface.

The voltages created at the potential electrodes are measured and the apparent resistivity of the subsurface material through which the current was transferred is determined using the standard electrical equation $V = I/R$. The depth of investigation is related to the spacing of the electrodes with larger spacings investigating deeper depths. For additional theory on the Wenner Array technique, see Ward, 1990 and Roy and Apparao, 1971.

The Wenner method was chosen because Ward (1990) suggests the technique has a high signal to noise ratio with a good resolution of horizontal layers, has a moderate rating for the resolution of steeply dipping structures (cracks) and is only moderately sensitive to surface inhomogeneities.

The Ground Penetrating Radar technique was chosen because of the very high resolution detection capabilities in the shallow subsurface and because of a broad range of experience with GPR signal responses at the SRS. GPR uses microwave range radar frequencies reflecting from subsurface changes in dielectric values to provide an

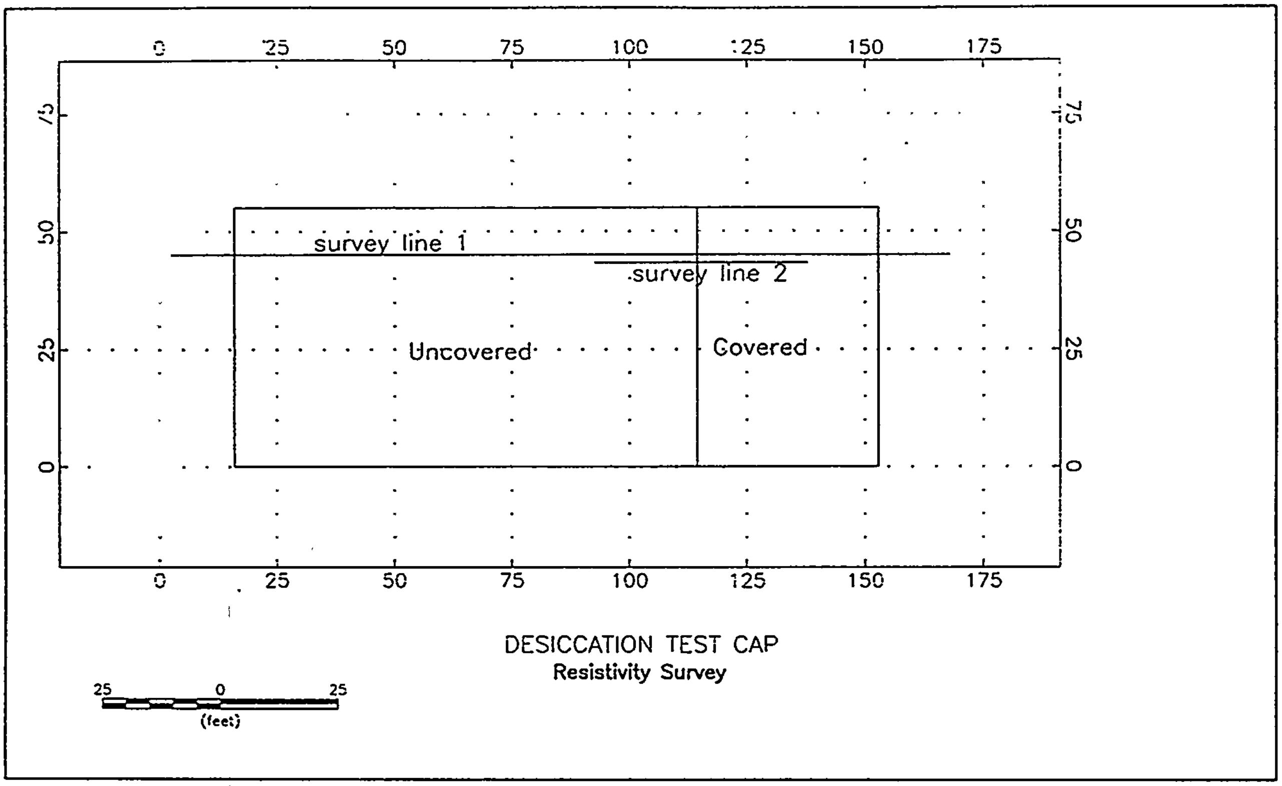

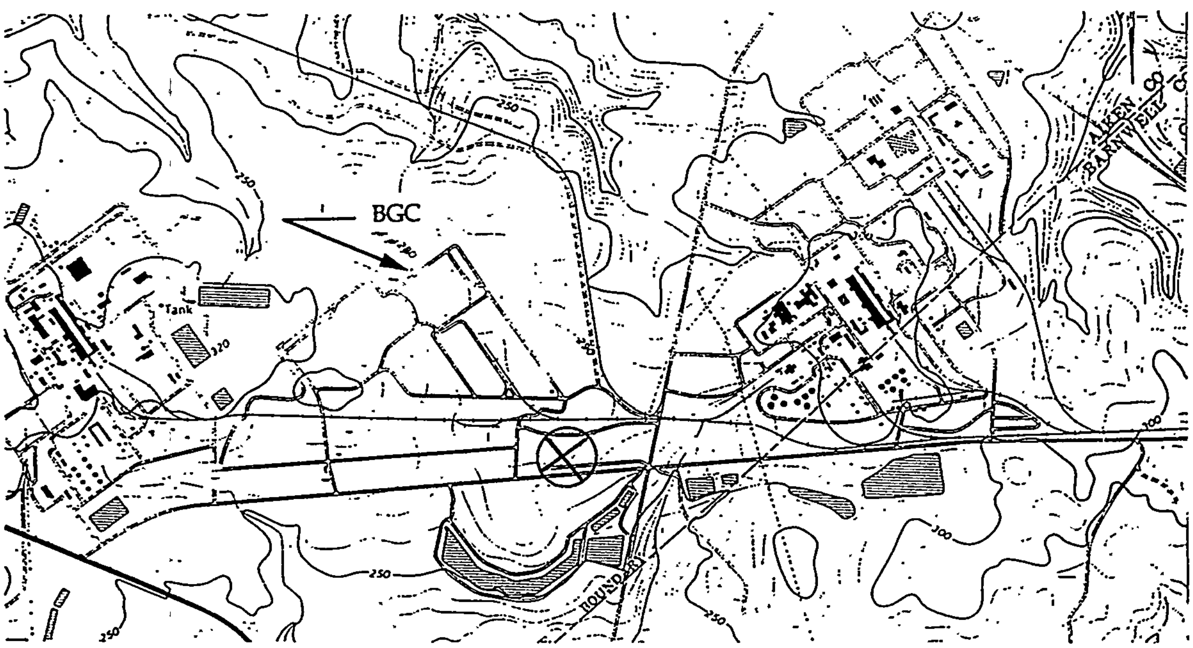

Figure 1. Plan view of the Desiccation Test Cap and survey lines. Resistivity data were acquired along Lines 1 and 2 and GPR data were acquired along Line 1. The Test Cap is located east of the Burial Ground Complex and along E Road.

electrical image of the subsurface. Basic GPR theory is discussed in Moffat and Puskar (1976), Ulriksen (1982), Davis and Annan (1989), Annan et al. (1991), Annan and Cosway (1992), Fisher et al. (1992), and Wyatt et al. (1993). Techniques for the seismic style processing of GPR data are discussed in Fisher et al. (1992b) and Hu et al. (1992). The use of multiple antenna frequencies is discussed in Smith and Jol (1992). Data were acquired in one sampling day therefore the overall seasonal variation of moisture remained steady throughout the study and the variations noted in Roberts et al. (1991) are not thought to affect the data.

The GSSI® 300 MHz antenna configuration was chosen for two principal reasons; 1) this antenna configuration (and the acquisition system) is readily available and commonly used, and 2) the 300 MHz frequency provides a shallower depth of investigation. The 450 MHz Pulse Ekko 1000® configuration was chosen because it is also readily available and commonly used while potentially providing shallower and higher resolution data than the 300 MHz configuration. The ability of the Pulse Ekko system to acquire data in a CMP mode also allowed for a seismic style imaging of the shallow subsurface.

It should be noted that both the resistivity and GPR measurements of the Desiccation Test Cap assume that the kaolin section, as originally engineered, was uniform and homogeneous. Therefore, any heterogeneities will be detected as anomalies. If there are natural variations in the uniformity of the kaolin section then it may not be possible to distinguish naturally occurring anomalies from the desired anomalies due to desiccation cracking.

METHODOLOGY

The initial survey line was established crossing the test cap from west to east. A zero station was established 17 feet west and 10 feet south of the uncovered kaolin cap. Flagged stations were set every 1.67 feet (0.51 m) until the cap was crossed with the final station placed 15 feet east of the test cap at a station 170 feet (51.8 m) from the start for a total of 100 sampling stations. Along this transect, the full thickness of the desiccation test cap exposed kaolin layer was reached at 71 feet (21.64 m), the covered (native soils and geotextile fabric) at 115 feet (35.05 m) and the edge of the test cap at 155 feet (47.2 m). This same transect was utilized for the GPR profiles. Figure 1 shows the transect line.

The Wenner data were acquired using an 'a' spacing of 1.67 ft (0.51 m). This 'a' spacing will generate apparent resistivities from a depth of approximately 1 foot (0.3 m). An ABEM Terrameter® with stainless steel electrodes was used to acquire the data. No attempt was made to actually determine a subsurface geophysical resistivity section by inversion. However, the data were used to generate a field of subsurface resistivity values to allow the graphical presentation of relative changes in subsurface conditions that may suggest cracking due to drying or structural failure. Terrameter® data were acquired using four cycles per sample with an input current of 0.5 milli-amperes. The data were reduced to apparent resistivities using the standard Wenner equation:

$$R_a = 2\pi\, a\, R_m$$

where a equals the 'a' spacing of 1.67 feet, R_m is the measured field resistivity and R_a is the apparent true resistivity, in ohm-feet, of the subsurface material.

The 450 MHz GPR data were acquired with Pulse Ekko 1000® system antenna configurations in parallel to direction of travel and perpendicular to direction of travel modes. The change in antenna orientation has been discussed as a method to evaluate high clay soils by preventing preferential polarization of clay particles by microwave induced currents. Additionally, data were acquired with the antenna arrays in contact and elevated from the ground surface. The use of antenna arrays elevated from the surface was an attempt to establish a clear 'T_0' time break to define a unique surface contact marker. Acquisition parameters for the 450 MHz array are described in Appendix B.

The third GPR technique used the SIR System 10 in a single channel mode with a fixed 300 MHz antenna. Data were acquired on the surface and in an elevated mode similar to the 450 MHz data. Acquisition parameters are discussed in Appendix B.

Processing of the GPR was kept to a minimum and was designed to eliminate systematic noise while maximizing the geologic signal. The processing of GPR data is further discussed in Appendix B.

RESULTS

The results of resistivity survey lines 1 and 2 are shown on Figures 2 and 3 respectively. Field data from the resistivity profiles are included in Appendix A. Maintaining the assumption that the resistivity array is measuring a uniform distance below surface (approximately 0.5 to 1 foot or 0.15 to 0.3 m) then an increase in resistivity is expected for the more impermeable clay layer (due to less interstitial water). Theoretically, if a discontinuity (open crack) exists between the potential electrodes (within the 1.67 foot or 0.51 m) then the resistivity will increase to infinity. In reality, the area of the apparent resistivity measurement is larger than the area of most cracks, therefore, a discontinuity would have to be complete across the area of the apparent resistivity to become infinite. Because of this, a general increase in resistivity above a predetermined level may suggest that discontinuous cracking is present. However, this increase may be caused by zones of drier clay and not be uniquely interpretable.

Within the full thickness of the uncovered test cap clay cover (refer to Figure 1) the average resistivity is approximately 1600 to 1700 ohm feet. This resistivity is apparently higher than the local soils, which is anticipated. Visual observation of the exposed kaolin demonstrated numerous desiccation cracks, similar to mud cracks, and a visible moisture profile was observable along the walls of the larger cracks. The clay had a higher moisture content a few centimeters below the surface but no cracks were observed to completely breach the clay (this was difficult to observe).

The covered portion of the clay cap exhibited a much higher resistivity probably due to less moisture below the plastic sheeting separating the cover material from the clay. Apparent resistivity values approached infinity for the western portion of the covered cap but it was not possible to distinguish whether this was from discontinuities or dryness in the clays. The eastern portion of the covered cap exhibited lower resistivities suggesting that more moisture was present beneath the soil cover and plastic. It was not possible to distinguish whether this was caused by more moisture in the clay beneath unobservable tears in the plastic or from a continuous clay layer with no discontinuities.

A second resistivity transect (Line 2) across the uncovered-to-covered interval was acquired one 'a' spacing south of the original transect (Line 1) in an attempt to verify the very high resistivity anomaly (refer to Figure 2). The results of this transect are shown on Figure 3. The average apparent resistivity is similar (approximately 1700 ohm feet) to Line 1 and the very high anomaly also appears to be present but shifted eastward. As with Line 1, there is a pronounced increase in resistivity under the soil and plastic cover possibly suggesting drier kaolin. The presence or absence of discontinuities or cracks is not discernible from this data and no definitive cause for the eastward shift could be determined. Since a definitive cause for the eastward shift in the data was not observable in the field, no additional transect lines were considered.

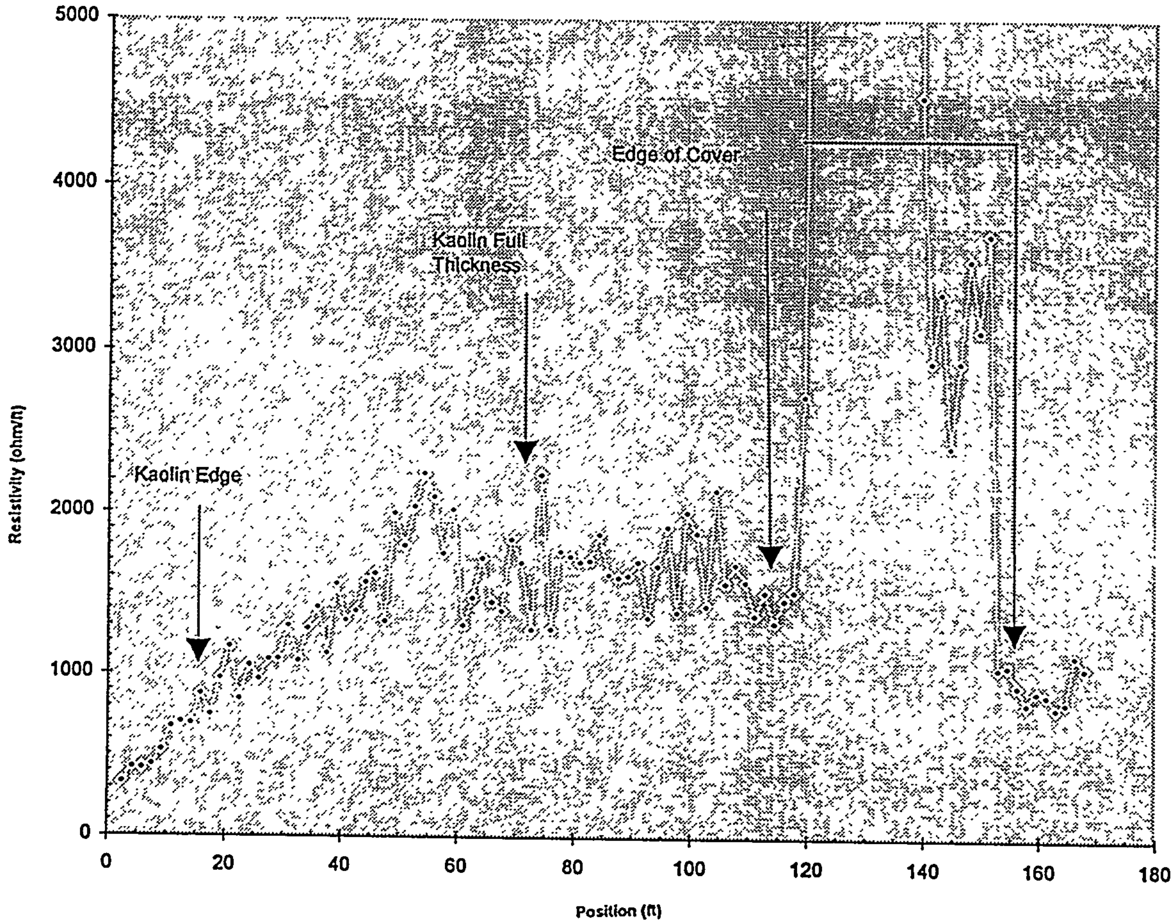

Figure 2. Results from Resistivity Line 1. Data are plotted as apparent resistivity versus distance along transect.

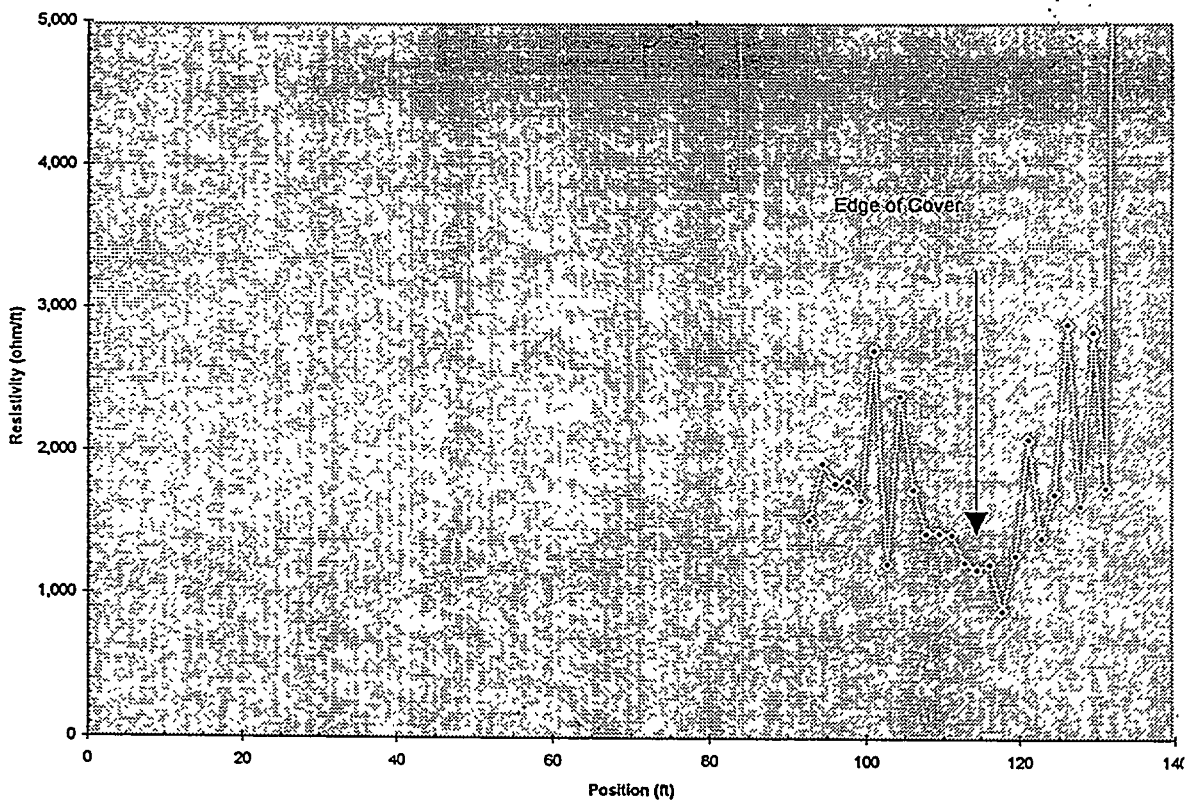

Figure 3. Results of Resistivity Line 2. Data are plotted as apparent resistivity versus distance along transect.

The results of the GPR surveys are mixed. As expected, the 300 MHz data images deeper zones but with less resolution than the 450 MHz data. The 300 MHz array images interpretable data to approximately 50 ns (6-7 feet or 2 m) while the 450 MHz array images to approximately 30 ns (4-5 feet or 1.5 m) (Figure 4). The overall configuration of the subsurface is similar between the two systems and frequencies but the GSSI® data (refer to Appendix B figures 19 and 20) is "ringier" or has a lower signal to noise ratio than the Pulse Ekko 1000®. Both frequency systems and antenna arrays were adequate to image the shallow clays within the test cap area. The inclined reflectors present on all sections (reference the Appendix B figures) are caused by the construction fill and sloping of the test cap which is gradual on the west and more abrupt on the east. Processing of the GPR data is discussed in Appendix B.

The response of the parallel versus perpendicular antenna arrays demonstrated a pronounced difference. The perpendicular array provides much better resolution with less signal noise suggesting a better couple with the subsurface and possibly less polarization. (Figure 5). The signal noise on the parallel array has the appearance of "wow" or ringing throughout the data suggesting that the processing required to eliminate the "wow" would eliminate the data as well. The spikes on the signal strength graphs at t_0, t_{12}, and t_{24} (nanoseconds) suggest that the "wow" has a periodicity of 12 ns ringing through the data while no such spikes are seen on the perpendicular graph. The presence of the clay beneath the cover is generally observable as a reflection package bounded on the top and bottom by a low amplitude reflections and with high amplitude internal reflections (Appendix B figure 2). A review of the data (note for example, figures 5, 6 and 9, included in Appendix B) demonstrates that there are no observable signal responses that uniquely suggest cracking or clay breaching within the interpreted clay interval.

The above ground acquisition established a clear t_o break, but lost too much energy due to scattering. Very little energy entered the subsurface allowing imaging to approximately 6 nanoseconds or less than one foot (0.3 m). The GPR signal was fully attenuated in the kaolin section, however, variations in attenuation and/or amplitude response within the clay (reference Appendix B figures 8 and 9 at depths of 8 to 10 ns) may be indicative of discontinuities or changes in uniformity. Further work will be necessary to determine if these anomalies are variations in moisture, clay thickness or composition or are structural features such as cracks.

CONCLUSIONS

In order for resistivity and GPR data to be adequately interpreted, it would be necessary to measure an undisturbed kaolin section to establish baseline resistivity values. Also, a breached section should be measured to establish the ideal response to a 'crack' or fracture in the clay. The use of resistivity to detect "wet" versus "dry" clay is highly possible, suggesting that resistivity may be a method of choice for locating places where the soil cover or plastic liner overlying the clay cap is breached. Generally, the lack of control on conditions under the covered portion of the test cap prevented the interpretation of the resistivity data to distinguish natural variations (such as those that may be due to heterogeneities in the clay) versus those that might be caused by cracks.

The results of the elevated ground penetrating radar surveys suggest that this technique may have promise as a "crack" detector. The 450 MHz GPR perpendicular array generated higher resolution data than the parallel array. The reasons for this will require a dedicated investigation but are probably related to orientation/anisotropy of the clay grains as deposited or may relate to preferential polarization and signal absorption based on the GPR microwave field orientation. The use of higher frequency GPR antenna configurations, possibly in the GHz range, used on the surface may detect small scale discontinuities in the kaolin. The use of 450 MHz or similar antenna systems, in an elevated mode so that the signal is attenuated within the zone of interest, may also be useful.

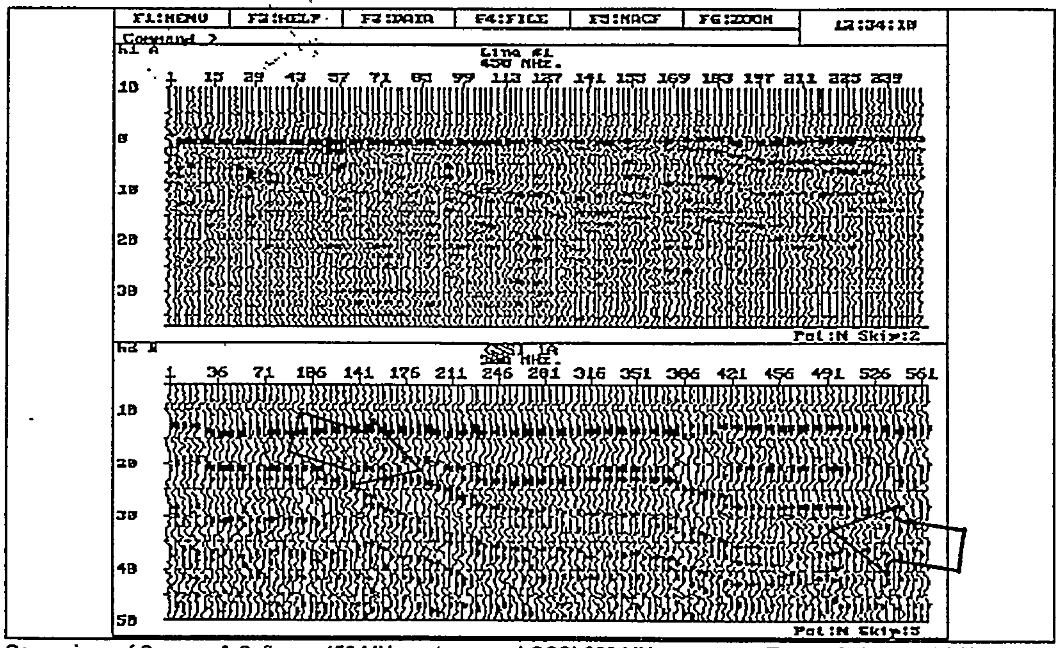

Comparison of Sensors & Software 450 MHz. antenna and GSSI 300 MHz. antenna. Top S&S, bottom GSSI.

Figure 4. Comparison of 450 MHz data to 300 MHz data, depth of investigation. The highlighted zone is the kaolin cap.

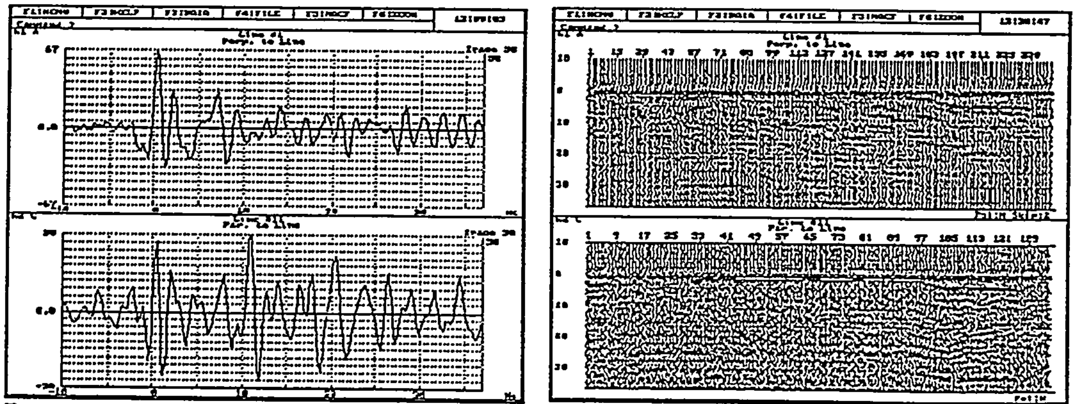

Top graph antennas orientated perpendicular to line. Bottom graph antennas orientated parallel to line.

Top section shot with antenna perpendicular to line. Bottom section has antenna parallel to line.

Figure 5. GPR response comparison of parallel versus perpendicular arrays. The signal to noise ratio of the data in the top figures suggest a better coupling of the perpendicular oriented GPR signal with the subsurface.

REFERENCES

Annan, A. P. and S. W. Cosway, 1992, "Ground Penetrating Radar Survey Design," *Proceedings of the Symposium on the Application of Geophysics to Engineering and Environmental Problems*, Vol. 2, Oakbrook, IL.

Annan, A. P., S. W. Cosway and J. D. Redman, 1991, "Water Table Detection with Ground Penetrating Radar," Expanded Abstracts, Vol. 1, pp. 494-495, Society of Exploration Geophysicists 61st Annual Meeting, Houston, TX.

Davis, J. L. and A. P. Annan, 1989, "Ground Penetrating Radar for High Resolution Mapping of Soil and Rock Stratigraphy," Geophysical Prospecting, Vol. 37, pp. 531-551.

Fisher, E., G. A. McMechan, and A. P. Annan, 1992, "Acquisition and Processing of Wide-Aperture Ground Penetrating Radar Data," Geophysics, Vol. 57, No. 3, p. 495-504.

Fisher, E., G. A. McMechan, A. P. Annan, and S. W. Cosway, 1992, "Examples of Reverse-Time Migration of Single-Channel Ground Penetrating Radar Profiles," Geophysics, Vol. 57, No. 4, pp. 577-586.

Hu, L. Z., M. Ramaswamy, and B. McCormick, 1992, "Delineate Subsurface Structures with Ground Penetrating Radar," Houston Advanced Research Center Report, p. 16.

Moffat, D. L. and R. J. Puskar, 1976, "A Subsurface Electromagnetic Pulse Radar," Geophysics. Vol. 41, No. 6, pp. 506-518.

Roberts, R., J. L. Daniels, and M. Vendl, 1991, "Seasonal Variations and Ground Penetrating Radar Data Repeatability," Expanded Abstracts, Vol. 1, pp. 486- 489, Society of Exploration Geophysicists 61st Annual Meeting, Houston, TX.

Roy, A. and A. Apparao, 1971, "Depth of Investigation in Direct Current Methods," Geophysics, Vol. 36, No. 5, pp. 943-959.

Smith, D. G. and H. M. Jol, 1992, "Ground Penetrating Radar Investigation of a Lake Bonneville Delta," Provo Level, Brigham City, UT, Geology, Vol. 20, pp. 1083-1086.

Ulriksen, C. P. F., 1982, "Application of Impulse Radar to Civil Engineering," Lund University of Technology, p.179.

Ward, S. H., 1990, "Resistivity and Induced Polarization Methods," Geotechnical and Environmental Geophysics, Vol. 1, S. H. Ward ed., pp. 147-189.

Wyatt, D. E., R. V. Brodine, G. B. Sexton, and R. J. Pirkle, 1993, "Advancements in Environmental Applications of Ground Penetrating Radar, In: Whitfield, P., Convenor, Meeting the Challenge, Environmental Remediation Conference, Proceedings of the ER '93, Environmental Remediation Conference, October 24-29, 1993, Augusta, GA.

Appendix A

Resistivity Data and Field Notes

This page intentionally left blank.

Test Cap Wenner Resistivity Profile #1 **Operator:D. Wyatt**

Date: 9-1-95

Comments: 85 deg, ground dry with some moisture, partly cloudy
array spacing = 5 feet, 'a' spacing = 1.67 feet

OBS	X	Y	Z-measured	Z-calc ohm/ft	Notes
1	2.51	45	31.6	332	use black wires for current, red for potential
2	4.18	45	40.3	423	arrive onsite 10:40 AM, begin survey 11:10AM
3	5.85	45	39.8	418	did not use reels
4	7.52	45	41.9	440	settings: 4 cycles, 5 mA,
5	9.19	45	50.6	531	incremental profile, move one MN each time
6	10.86	45	64.4	676	start at 0 ft, 17' kaolin, full kaolin thickness @ 71'
7	12.53	45	67	703	edge of cover & plastic @115', ending edge of cover (to east) @ 155', end line @ 170'
8	14.20	45	66.3	696	all notes measured from center of potential electrodes
9	15.87	45	83.7	878	edge of kaolin
10	17.54	45	71.5	750	
11	19.21	45	92.7	973	cracks 1-2 mm
12	20.88	45	111.2	1,167	
13	22.55	45	80.5	845	
14	24.22	45	100.3	1,052	damp clay
15	25.89	45	92.3	968	
16	27.56	45	103.8	1,089	
17	29.23	45	104.1	1,092	
18	30.90	45	123.7	1,298	wider dessication cracks up to 1 cm
19	32.57	45	102.9	1,080	
20	34.24	45	122.1	1,281	
21	35.91	45	134.6	1,412	
22	37.58	45	107.3	1,126	
23	39.25	45	148.2	1,555	
24	40.92	45	127	1,333	
25	42.59	45	132.4	1,389	
26	44.26	45	149.2	1,566	
27	45.93	45	154.4	1,620	
28	47.60	45	126.5	1,327	move spread
29	49.27	45	190.3	1,997	
30	50.94	45	171	1,794	
31	52.61	45	194.2	2,038	
32	54.28	45	214	2,245	more polarization noted
33	55.95	45	200	2,099	more polarization noted
34	57.62	45	166.6	1,748	more polarization noted
35	59.29	45	192.4	2,019	more polarization noted
36	60.96	45	124.2	1,303	more polarization noted
37	62.63	45	140.1	1,470	

38	64.30	45	164	1,721	
39	65.97	45	138.1	1,449	
40	67.64	45	132.8	1,393	
41	69.31	45	174.9	1,835	
42	70.98	45	161.2	1,691	edge of kaolin cap, west rope edge from photo
43	72.65	45	121.7	1,277	
44	74.32	45	213	2,235	
45	75.99	45	122	1,280	
46	77.66	45	168	1,763	
47	79.33	45	165.1	1,732	more polarization noted
48	81.00	45	161.8	1,698	more polarization noted
49	82.67	45	162.4	1,704	more polarization noted
50	84.34	45	178.2	1,870	
51	86.01	45	154.2	1,618	
52	87.68	45	152.5	1,600	
53	89.35	45	153.7	1,613	
54	91.02	45	162	1,700	rope center of cap from photo
55	92.69	45	129.1	1,355	
56	94.36	45	159.5	1,674	move spread
57	96.03	45	182.8	1,918	
58	97.70	45	132.6	1,391	
59	99.37	45	191.1	2,005	
60	101.04	45	179	1,878	
61	102.71	45	136	1,427	
62	104.38	45	204	2,141	
63	106.05	45	149.2	1,566	
64	107.72	45	160.4	1,683	
65	109.39	45	150.2	1,576	
66	111.06	45	130.5	1,369	east rope edge
67	112.73	45	143.9	1,510	
68	114.40	45	126.1	1,323	east edge of plastic and cover
69	116.07	45	139.3	1,462	
70	117.74	45	144.2	1,513	current would not penetrate platic, had to drive electrodes below plastic
71	119.41	45	259	2,718	
72	121.08	45	1181	12,392	high polarization
73	122.75	45	5470	57,396	
74	124.42	45	1002	10,514	
75	126.09	45	952	9,989	
76	127.76	45	2740	28,751	
77	129.43	45	1532	16,075	
78	131.10	45	1824	19,139	
79	132.77	45	1633	17,135	
80	134.44	45	1503	15,771	
81	136.11	45	605	6,348	
82	137.78	45	2110	22,140	
83	139.45	45	432	4,533	move spread
84	141.12	45	279	2,928	

85	142.79	45	319	3,347	
86	144.46	45	230	2,413	
87	146.13	45	279	2,928	
88	147.79	45	338	3,547	
89	149.46	45	297	3,116	
90	151.13	45	353	3,704	
91	152.80	45	99.9	1,048	edge of cap
92	154.47	45	101.2	1,062	
93	156.14	45	89.6	940	
94	157.81	45	79.6	835	
95	159.48	45	86.3	906	off of backfill
96	161.15	45	84.5	887	lots of weeds on electrodes
97	162.82	45	76.9	807	
98	164.49	45	80.1	840	
99	166.16	45	107.4	1,127	
100	167.83	45	99.8	1,047	end at 170', time is 1 pm
1	92.69	43.3	144.8	1,519	start at 90', end at 140', moved south one MN spacing
2	94.36	43.3	182.2	1,912	stat at 1/2 distance rope across exposed clay, start at 1:10pm
3	96.03	43.3	169.3	1,776	
4	97.70	43.3	170.7	1,791	
5	99.37	43.3	158	1,658	
6	101.04	43.3	258	2,707	
7	102.71	43.3	116	1,217	
8	104.38	43.3	227	2,382	
9	106.05	43.3	165.2	1,733	
10	107.72	43.3	135.9	1,426	
11	109.39	43.3	136.2	1,429	
12	111.06	43.3	135.3	1,420	eastern rope for pix
13	112.73	43.3	116.8	1,226	
14	114.40	43.3	112.1	1,176	edge of plastic
15	116.07	43.3	115.6	1,213	
16	117.74	43.3	84.7	889	
17	119.41	43.3	121.6	1,276	
18	121.08	43.3	198.8	2,086	
19	122.75	43.3	133.2	1,398	polarization
20	124.42	43.3	162.3	1,703	
21	126.09	43.3	275	2,886	
22	127.76	43.3	154.5	1,621	
23	129.43	43.3	270	2,833	
24	131.10	43.3	166.5	1,747	
25	132.77	43.3	863	9,055	
26	134.44	43.3	1346	14,123	
27	136.11	43.3	1178	12,361	
28	137.78	43.3	1793	18,814	end at 1:35pm

Appendix B

Microseeps® GPR Data and Report

This page intentionally left blank.

Final Report

GROUND PENETRATING RADAR INVESTIGATIONS

at the

CLAY CAP TEST SITE

SAVANNAH RIVER SITE

October, 1995

G.Boyd Sexton
Robert J. Pirkle

As a Part of
Proposal No. SOS140EC

EXECUTIVE SUMMARY

A Ground Penetrating Radar (GPR) survey was executed on October 3, 1995 at the Clay Cap Test Site for the purpose of determining if high frequency radar signals could locate small fractures in the clay and if radar antenna orientation is critical in determination. The survey yielded good GPR data, however all planned antenna configurations could not be run due to inclement weather produced by hurricane Opal.

TABLE OF CONTENTS

LIST OF TABLES

LIST OF FIGURES
CLAY CAP TEST SITE

LIST OF FIGURES (con't.)

CLAY CAP TEST SITE

I. INTRODUCTION

A Ground Penetrating Radar (GPR) survey was run at the Clay Cap Test Site for the purpose of determining if desiccation cracks or fractures could be seen beneath the clay cap covering the test site and amount of penetration of the signal beneath the clay cover. Various antenna orientations were planned to be conducted to determine the polarizating effect of the radar signal. The Clay Cap Test Site had a resistivity survey conducted prior to the GPR survey. The flagged survey stakes which were used in the resistivity survey were used as starting and ending points during the GPR survey. The distance between the stakes was 165 feet. All GPR lines were run along the same line starting at 13 feet and ending at 161 feet. All GPR lines have vertical marks displayed on the sections indicating the points where the antennas crossed the rope grid used as reference points. Due to cable length the last few feet on either end of the line were not surveyed.

II. BACKGROUND AND OBSERVATIONS

The Clay Cap Test Site is due east of the Burial Ground and fronting Road "E". The area has various experimental and testing sites within a large expanse. This project area is one small area within other test sites. The Clay Cap Test Site is a miniature version of a trench with a clay cap that might be typical in the Burial Ground. The weather during field acquisition was warm and overcast. The evening of October 3, rain started from hurricane Opal and continued for the next several days. Personnel on-site during data acquisition were Boyd Sexton and Mike Woodward of Microseeps. Randy Cumbest of WSRC was present during the initial phases of acquisition.

III. ACQUISITION AND PROCESSING PARAMETERS

The equipment and software used in the acquisition and processing of the GPR data are listed on Table 2. Both the Sensors and Software Pulse Ekko 1000 and GSSI Sir 10 System were employed. The antennas with Sensors and Software 1000 were 225, 450 and 900 MHz.. Due to weather conditions at the site only the S&S 450 MHz. and GSSI 300 MHz. antenna were used. The survey wheel was not used with the S&S system so each line has varying numbers of traces, but vertical ticks are placed where the rope boundaries were crossed.

Antenna orientation with the S&S is described in the diagram below:

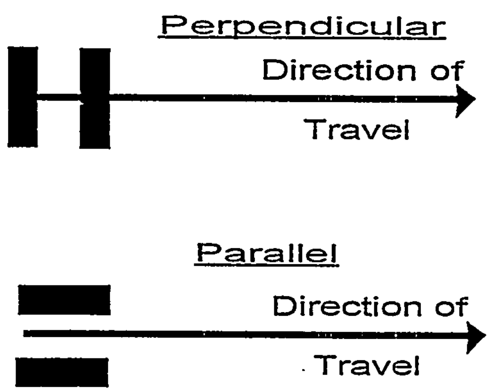

The final plots of all GPR data have the following processing routines applied.

S&S Data

AGC
SPIKING DECON
AGC
FK FILTER
MEAN FILTER

GSSI Data

SPIKING DECON
AGC
FK FILTER
MEAN FILTER

IV. RESULTS

The results of the GPR surveys at Clay Cap Test Site are shown on Figures 4 - 22. A sample GPR section with labeled interpretive information is shown on Figure 2. Typical signatures of an air wave, ground surface and subsurface features are labeled so that similar anomalous areas on the actual lines presented on Figures 4 - 22 can be easily recognized. The acquisition and processing information can be found on Table 2. The radar velocity in this area is 6-7 ns per foot.

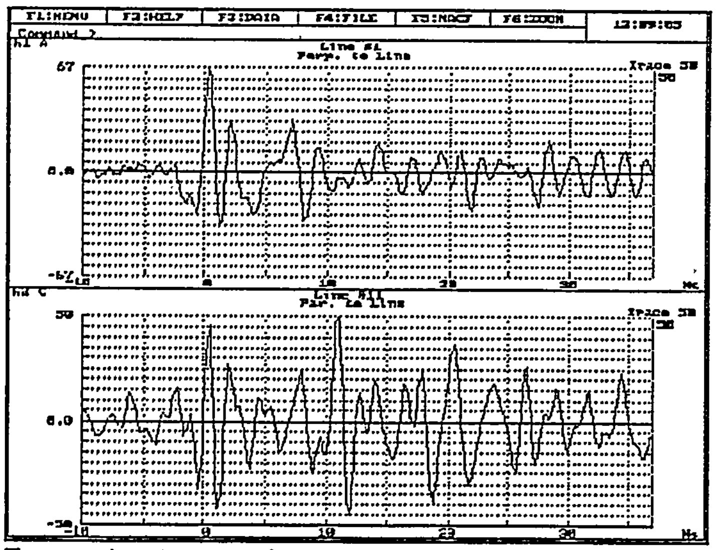

Top graph antennas orientated perpendicular to line. Bottom graph antennas orientated parallel to line.

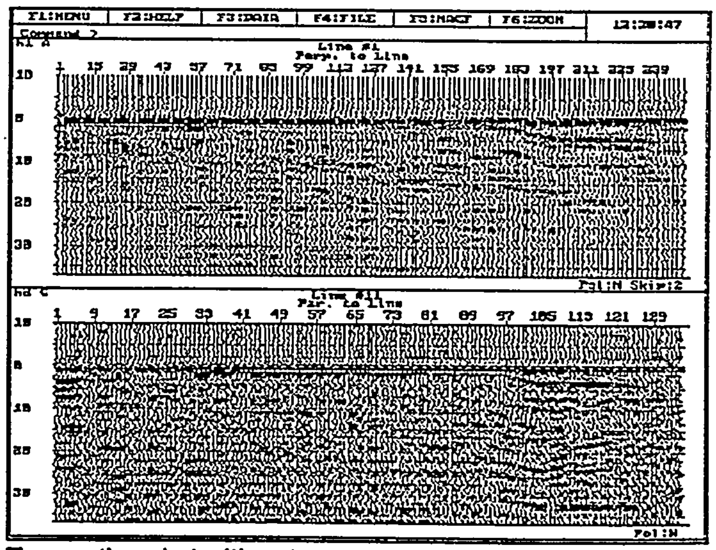

Top section shot with antenna perpendicular to line. Bottom section has antenna parallel to line.

The Clay Cap Test Site was generally a good data area. The above plots compare the perpendicular versus parallel data acquired with the S&S 450 MHz antenna. Clearly the perpendicular antenna array has better definition than the parallel configuration. The parallel configuration appears to generate higher amplitude noise spikes as seen on the upper left graph.

"Air shooting" (with antennas off the ground) was tried on lines 5,6,9,10,13,14,15 and 16. The purpose was to define the actual air/ground contact and hopefully see any indications of the desiccation fractures at the air/ground surface. This test had limited successs, possibly due to the high loss of energy through the air. As can be seen in these plots little energy is reflected from the subsurface.

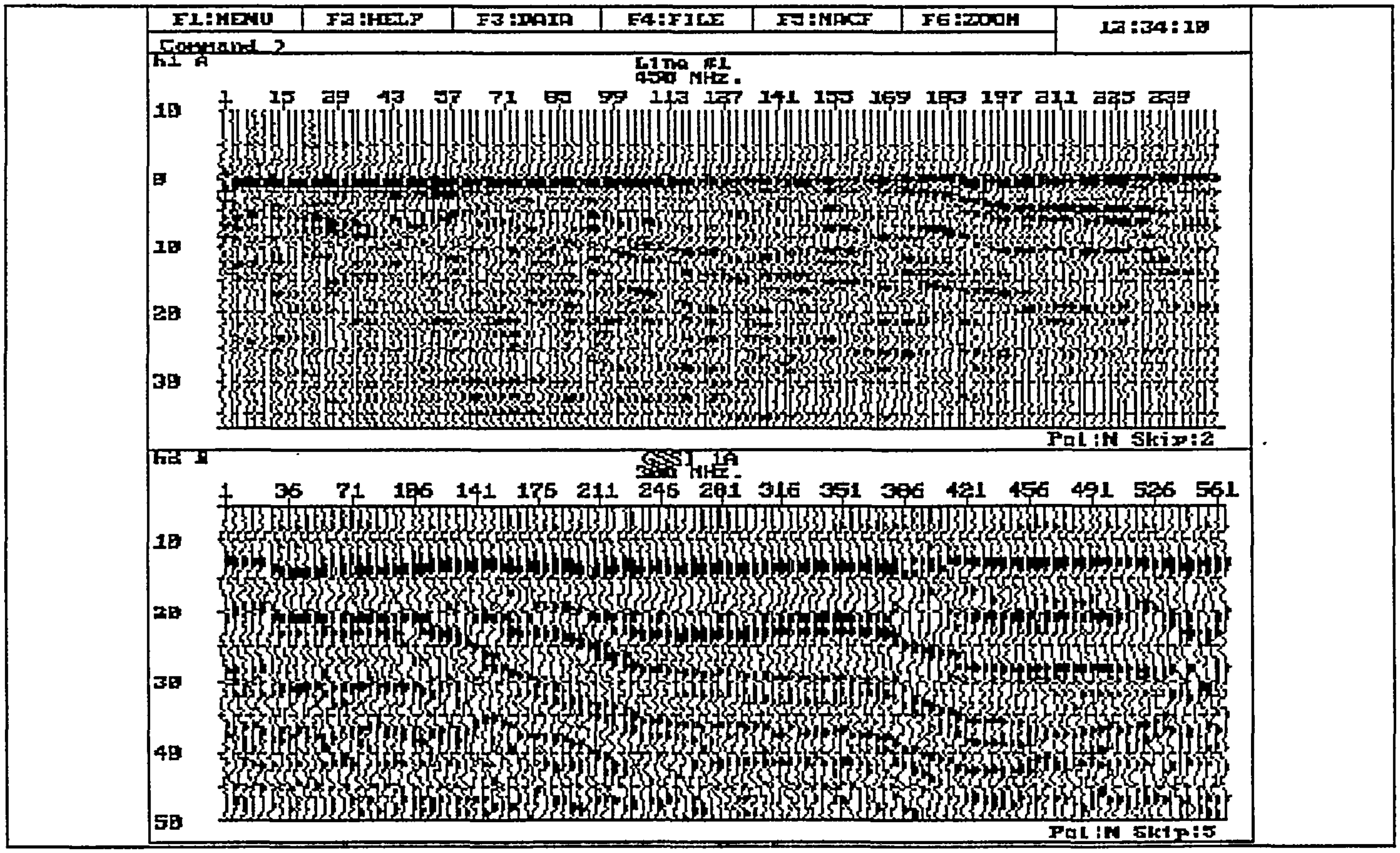

Comparison of Sensors & Software 450 MHz. antenna and GSSI 300 MHz. antenna. Top S&S, bottom GSSI.

Good subsurface details can be seen in many of the plots with amplitude contrasts which could be indicative of moisture/clay content. The comparison between S&S 450 MHz. and GSSI 300 MHz is as expected with the 300 MHz. penetrating deeper, but with slightly less resolution as compared to the 450 MHz. antenna.

V. CONCLUSIONS

The quality of the data recorded at Clay Cap Test Site was good. The data appears to show the clay being very susceptible to the orientation of the antennas. Ground contact by the antennas is critical, possibly more so in higher frequency antennas which were used on this project.

TABLE #1
CLAY CAP TEST SITE
TABLE OF COORDINATES, BEARINGS, AND DISTANCES

FIGURE	LINE NAME	X EASTING	Y NORTHING	BEARING	DISTANCE	LINE
4	1	No site coordinates could be obtained for the			149	1
5	2	HP (Orange Balls) hence no site coordinates			149	2
6	3	can be computed for GPR lines.			149	3
7	4				149	4
8	5				149	5
9	6				149	6
10	7				149	7
11	8				149	8
12	9				149	9
13	10				149	10
14	11				149	11
15	12				149	12
16	13				149	13
17	14				149	14
18	15				149	15
19	16				149	16
20	1A				149	1A
21	2A				149	2A

TOTAL FOOTAGE IN SURVEY	2682
TEST FOOTAGE NOT SHOWN	443
PROJECT TOTAL FOOTAGE	**3125**

Table 2

Acquisition and Processing Parameters

at the

Clay Cap Test Site

S&S

Date Data Acquired	10/3/95
Instrument Type	Pulse Ekko 1000
Antenna Type	450 Bi-Static
Range	Varied 50-100 ns
Pulse Voltage	200 Volts
Processing	Dewow, Dephase, AGC, Spiking Decon, AGC, Fk Filter, Mean Filter

GSSI

Date Data Acquired	10/3/95
Instrument Type	GSSI (SIR 10) S/N 1158
Antenna Type	100 MHz Mono-Static
Calibration Numbers	Supplied by GSSI PG-90-177 Version 2.05 Max 141 Min 20 Diff 121
Post Processing Software	GSSI (RADANIII), SIS Vista GPR
Range	250 ns
Start Position	-40 ns
End Position	210 ns
Survey Wheel	131.06 ticks/foot
Scans/Foot	2
Samples/Scan	512
Transmit Pulse Rate	50 Khz
Vertical IIR Low Pass Filter	N=2 F=50
Vertical IIR High Pass Filter	N=2 F=6
Horizontal Low Pass Filter	TC=0
Processing	Spiking Decon, AGC, Fk Filter, Mean Filter

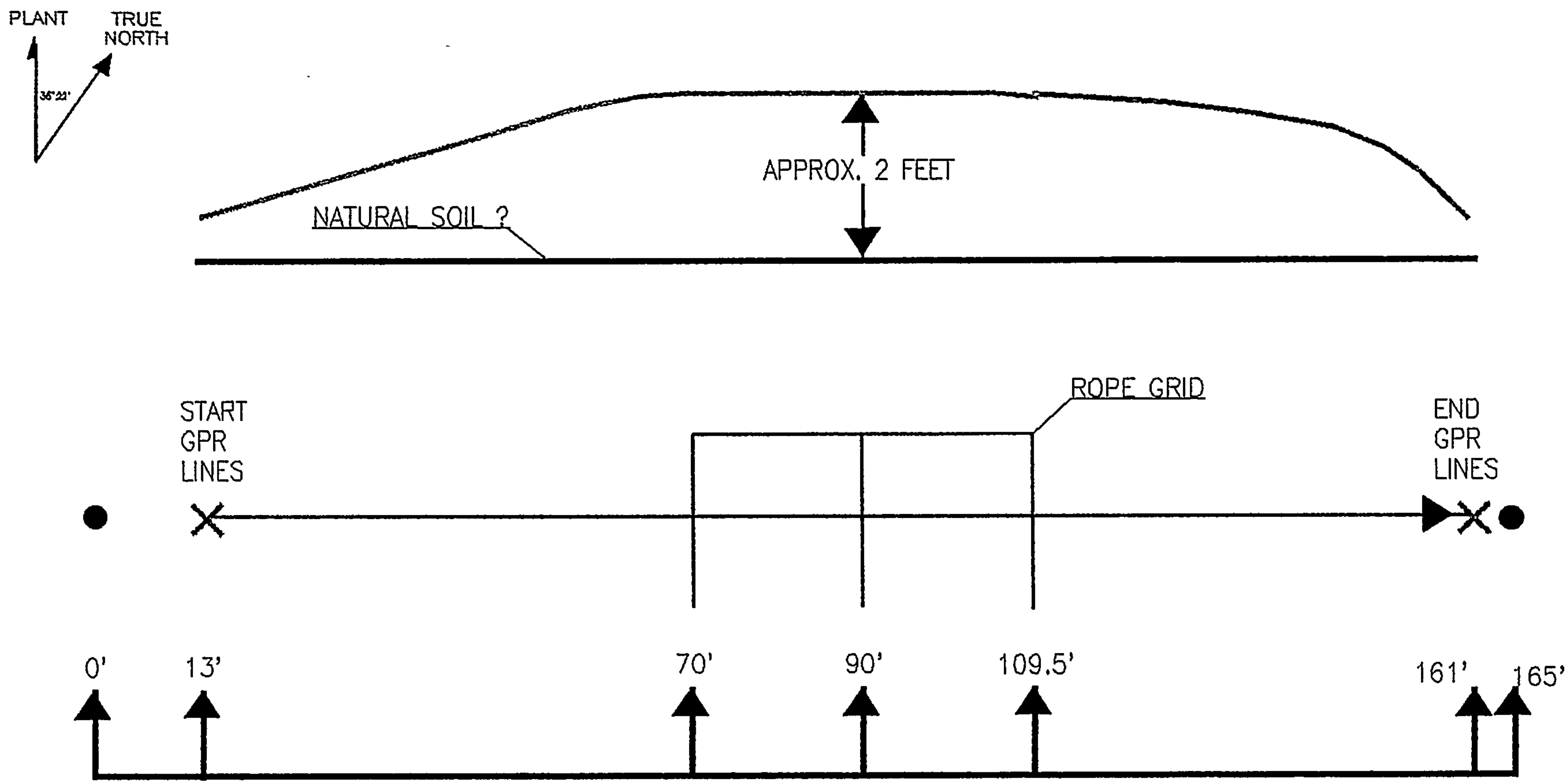

LEGEND

- ● OLD FLAGGED STAKE
- ✕ START/END POINTS GPR LINES
- → GPR LINE WITH DIRECTION
- —— CLAY MATERIAL
- —— MAT MATERIAL

0' 10' 20' 40 FEET

SAVANNAH RIVER SITE CLAY CAP TEST SITE GPR SURVEY FIGURE 2
TITLE: SITE LOCATION MAP DATE: OCTOBER, 1995
AREA: TEST SITE BESIDE BURIAL GROUND
PREPARED BY: [illegible], PITTSBURGH PA

FIGURE 1

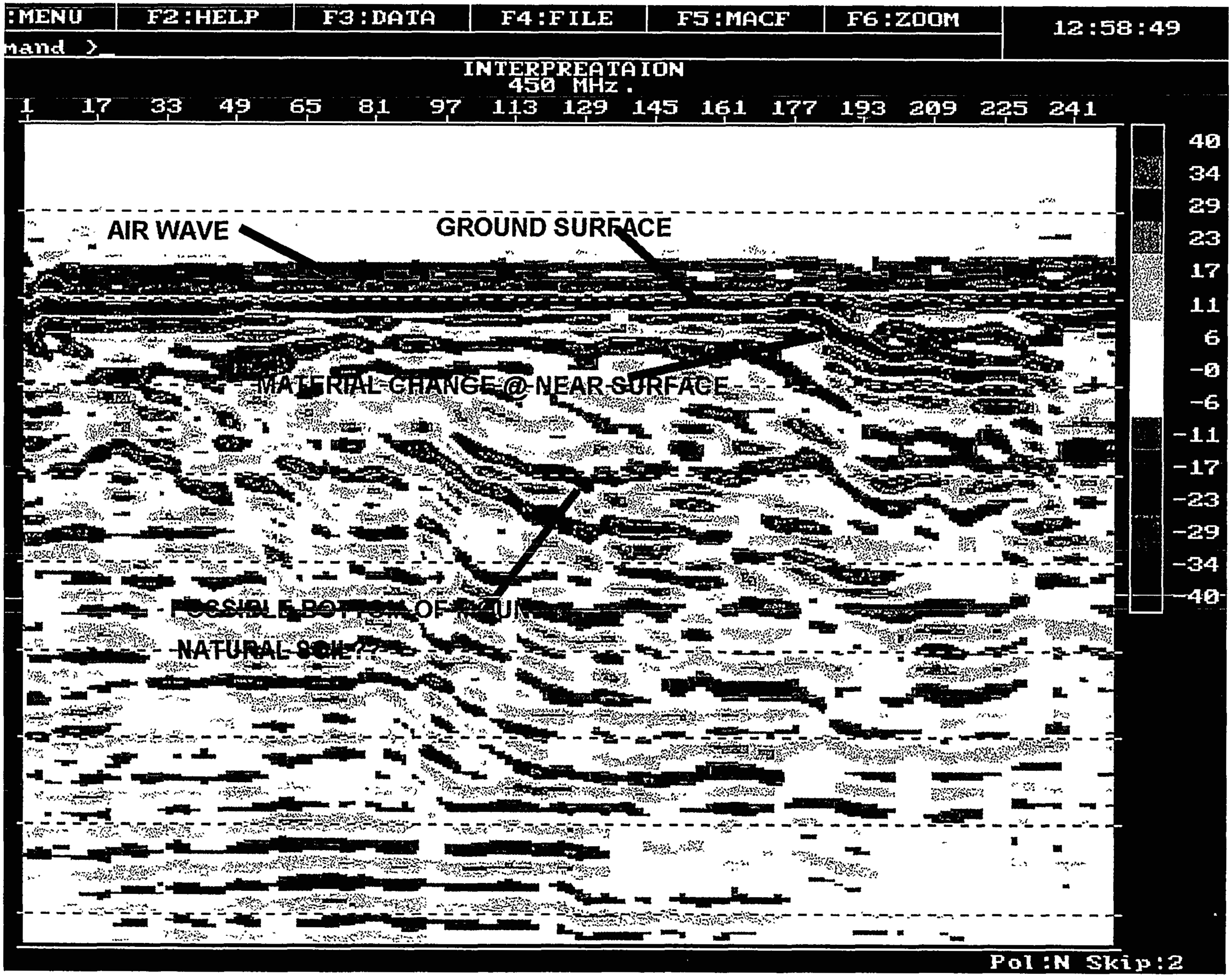

:MENU
F2:HELP
F3:DATA
F4:FILE
F5:MACF
F6:ZOOM
12:58:49
mand >
INTERPREATAION
450 MHz.
1 17 33 49 65 81 97 113 129 145 161 177 193 209 225 241
40 34 29 23 17 11 6 -0 -6 -11 -17 -23 -29 -34 -40
AIR WAVE
GROUND SURFACE
MATERIAL CHANGE @ NEAR SURFACE
NATURAL SOIL??
Pol:N Skip:2

FIGURE 2

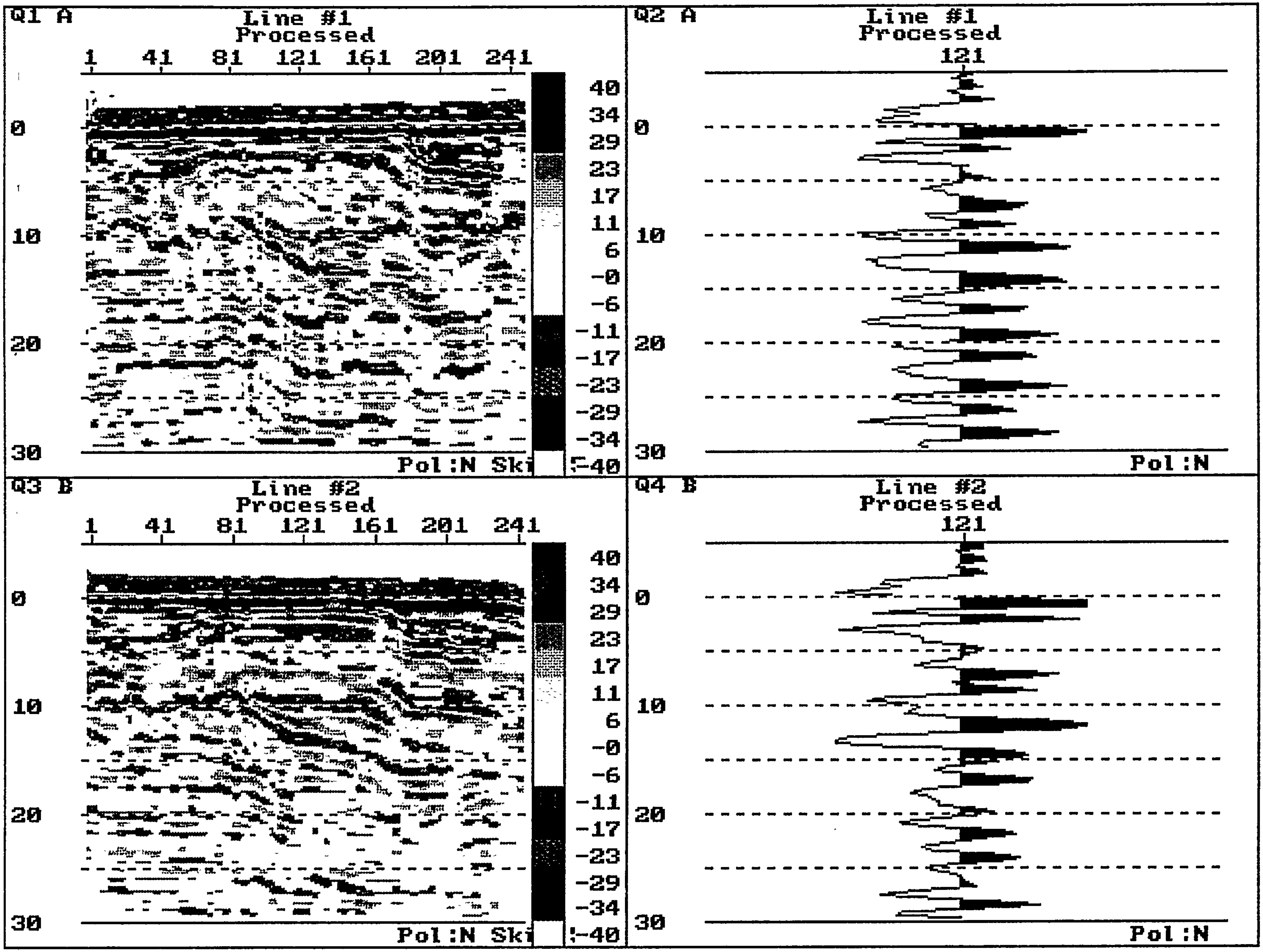

Q1 A
Line #1
Processed
1 41 81 121 161 201 241
0
10
20
30
40 34 29 23 17 11 6 -0 -6 -11 -17 -23 -29 -34 -40
Pol:N Ski
Q2 A
Line #1
Processed
121
0
10
20
30
Pol:N
Q3 B
Line #2
Processed
1 41 81 121 161 201 241
0
10
20
30
40 34 29 23 17 11 6 -0 -6 -11 -17 -23 -29 -34 -40
Pol:N Ski
Q4 B
Line #2
Processed
121
0
10
20
30
Pol:N

FIGURE 3

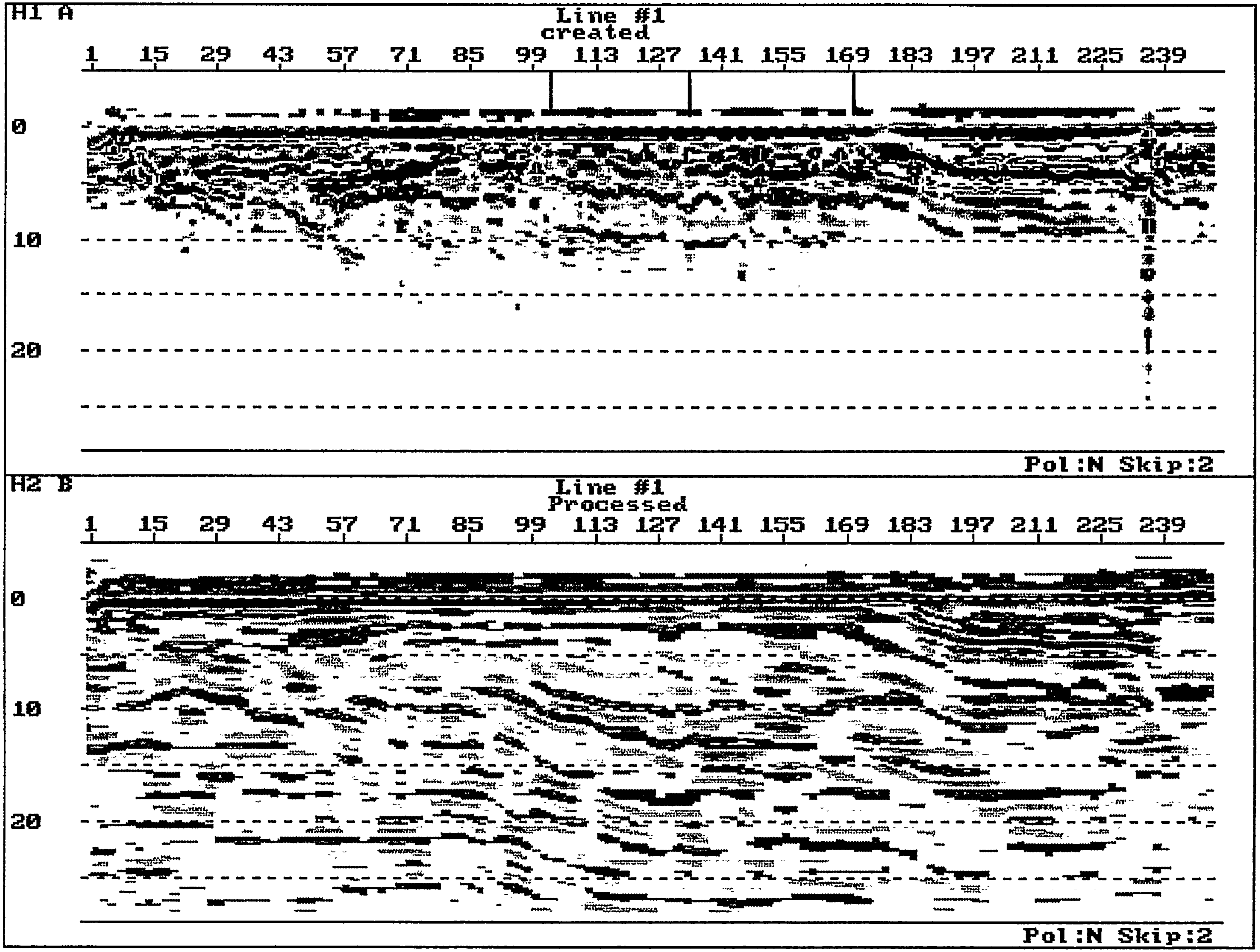
H1 A
Line #1
created
1 15 29 43 57 71 85 99 113 127 141 155 169 183 197 211 225 239
0
10
20
Pol:N Skip:2
H2 B
Line #1
Processed
1 15 29 43 57 71 85 99 113 127 141 155 169 183 197 211 225 239
0
10
20
Pol:N Skip:2

FIGURE 4

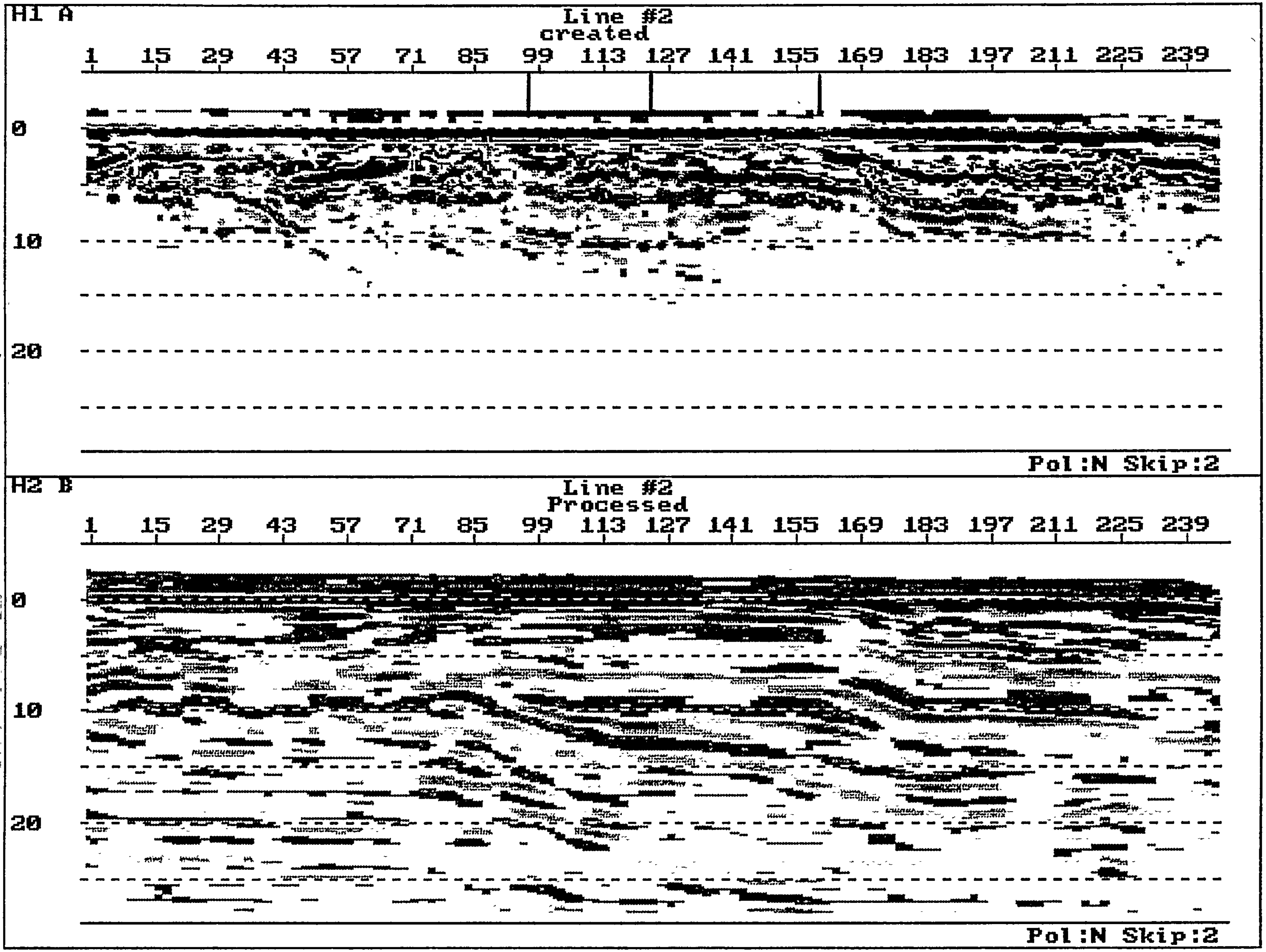
H1 A
Line #2
created
1 15 29 43 57 71 85 99 113 127 141 155 169 183 197 211 225 239
0
10
20
Pol:N Skip:2
H2 B
Line #2
Processed
1 15 29 43 57 71 85 99 113 127 141 155 169 183 197 211 225 239
0
10
20
Pol:N Skip:2

FIGURE 5

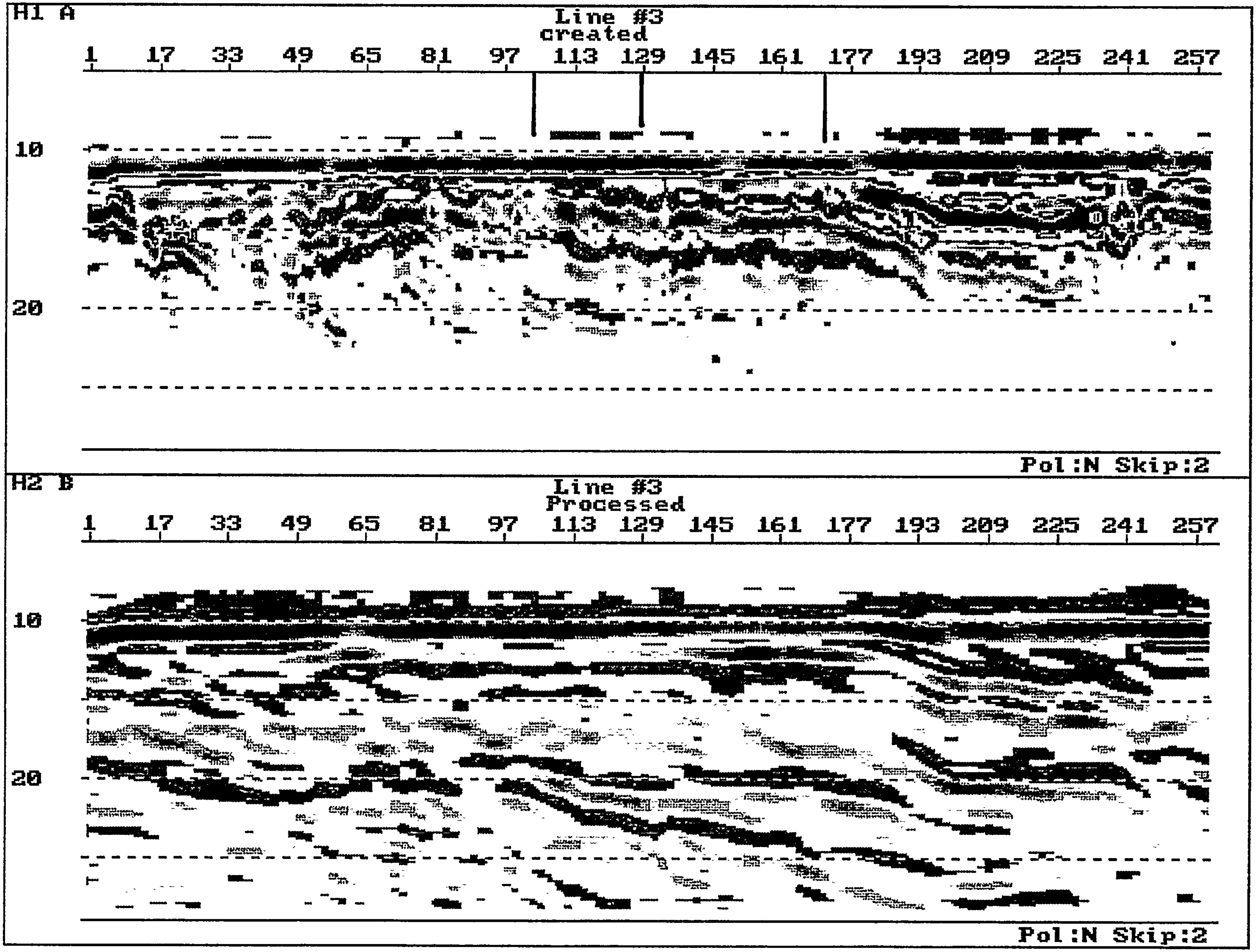
H1 A
Line #3
created
1 17 33 49 65 81 97 113 129 145 161 177 193 209 225 241 257
10
20
Pol:N Skip:2
H2 B
Line #3
Processed
1 17 33 49 65 81 97 113 129 145 161 177 193 209 225 241 257
10
20
Pol:N Skip:2

FIGURE 6

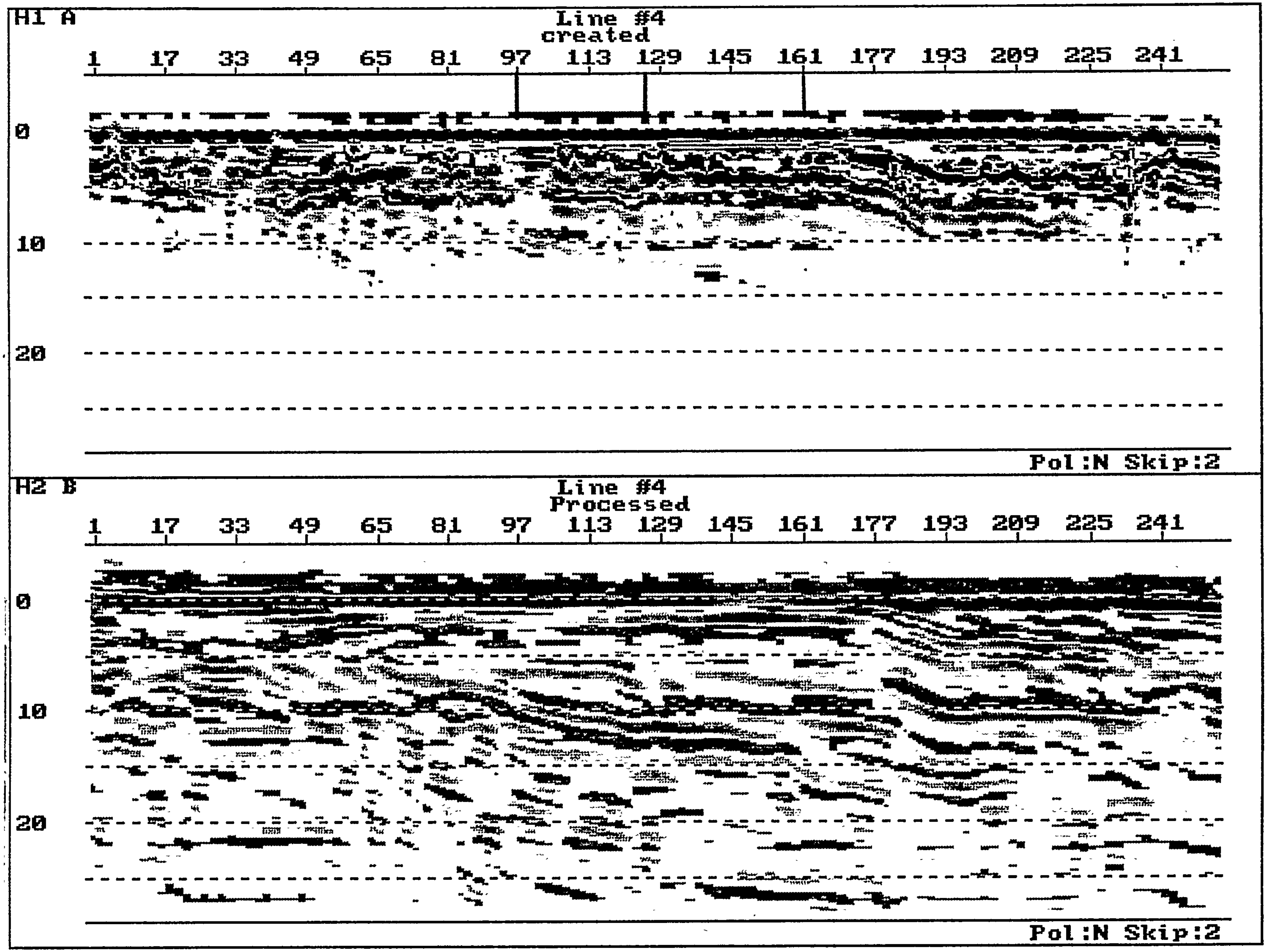

H1 A
Line #4
created
1 17 33 49 65 81 97 113 129 145 161 177 193 209 225 241
0
10
20
Pol:N Skip:2
H2 B
Line #4
Processed
1 17 33 49 65 81 97 113 129 145 161 177 193 209 225 241
0
10
20
Pol:N Skip:2

FIGURE 7

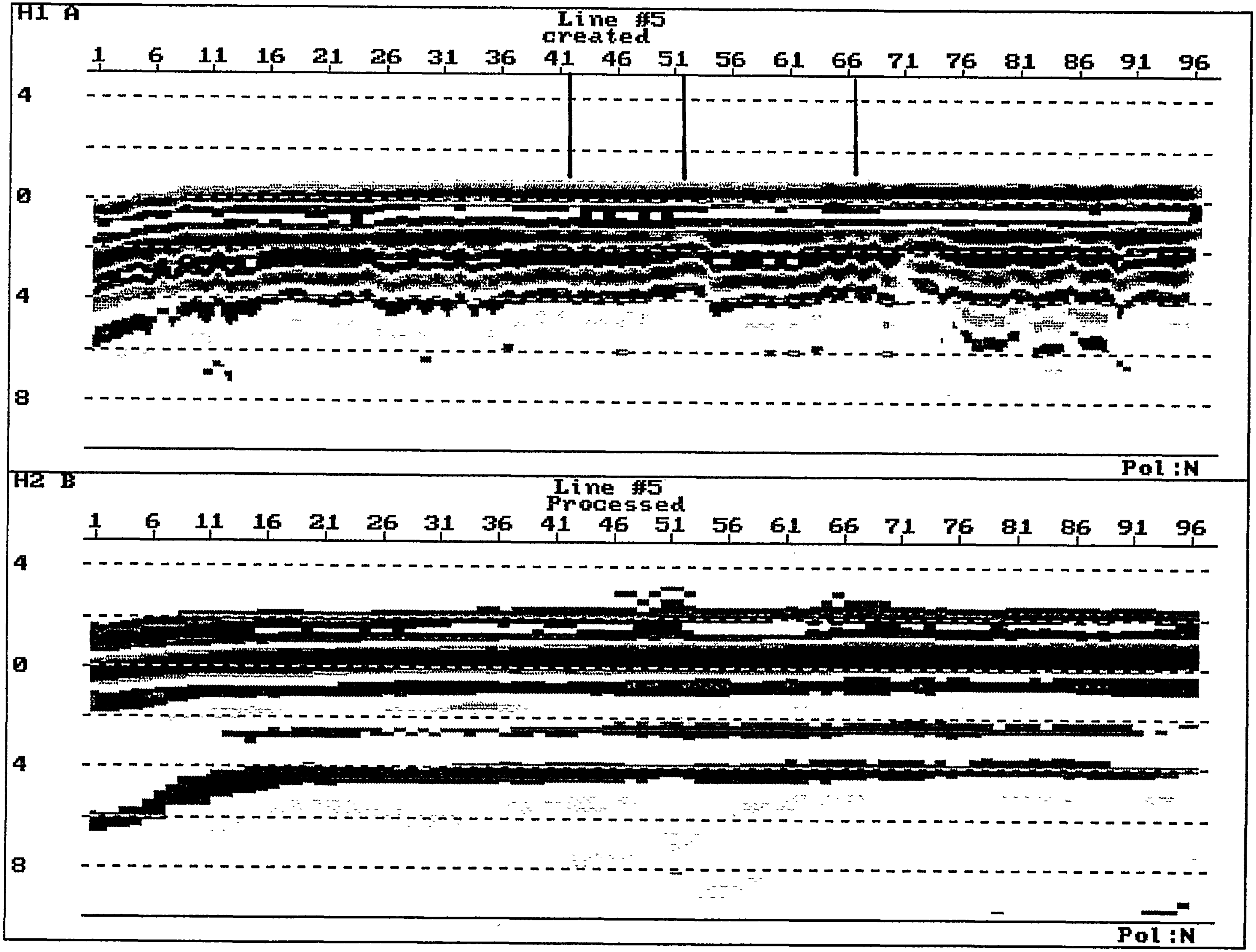
H1 A
Line #5
created
1 6 11 16 21 26 31 36 41 46 51 56 61 66 71 76 81 86 91 96
4
0
4
8
Pol:N
H2 B
Line #5
Processed
1 6 11 16 21 26 31 36 41 46 51 56 61 66 71 76 81 86 91 96
4
0
4
8
Pol:N

FIGURE 8

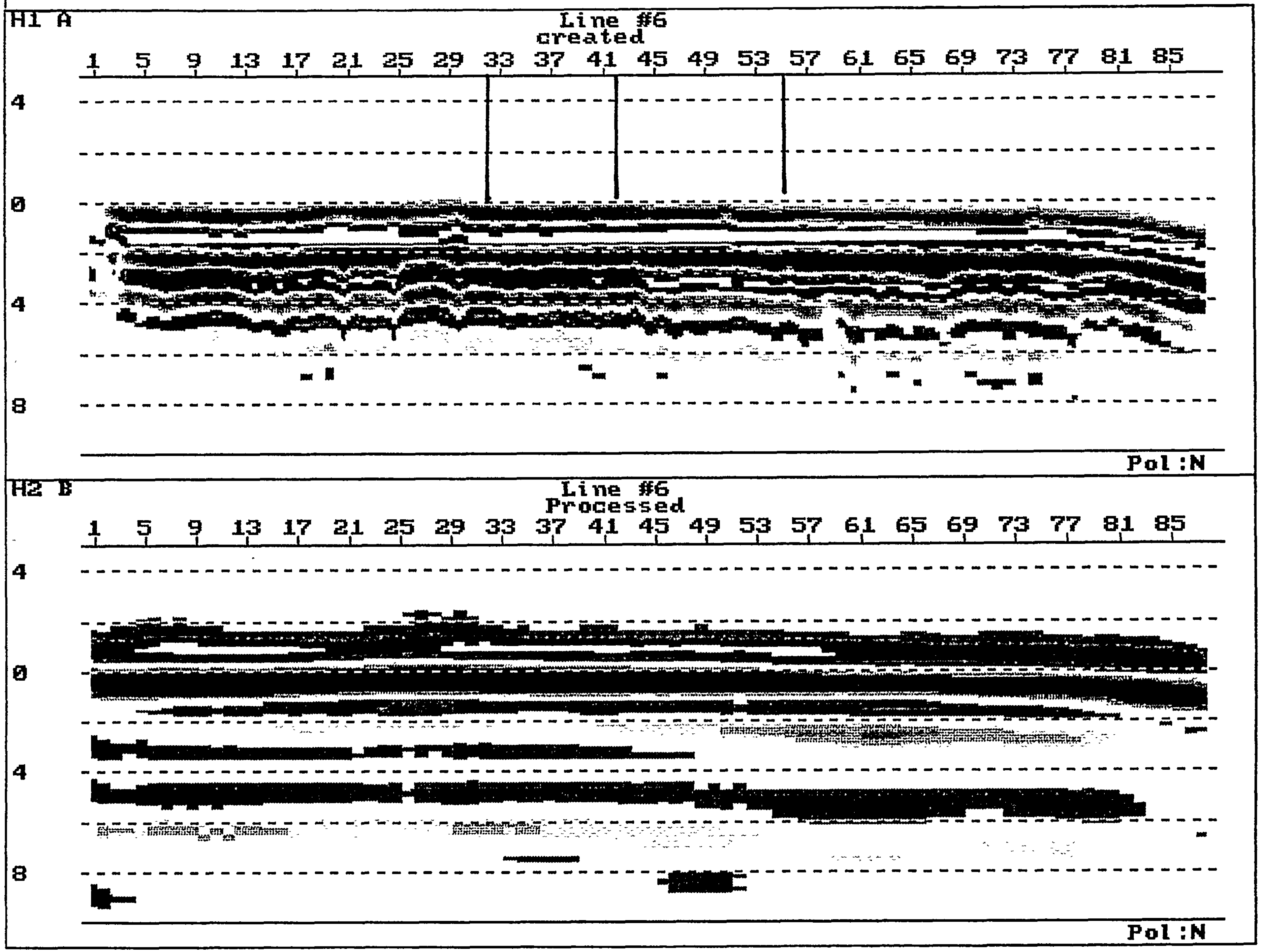
H1 A
Line #6
created
1 5 9 13 17 21 25 29 33 37 41 45 49 53 57 61 65 69 73 77 81 85
4
0
4
8
Pol:N
H2 B
Line #6
Processed
1 5 9 13 17 21 25 29 33 37 41 45 49 53 57 61 65 69 73 77 81 85
4
0
4
8
Pol:N

FIGURE 9

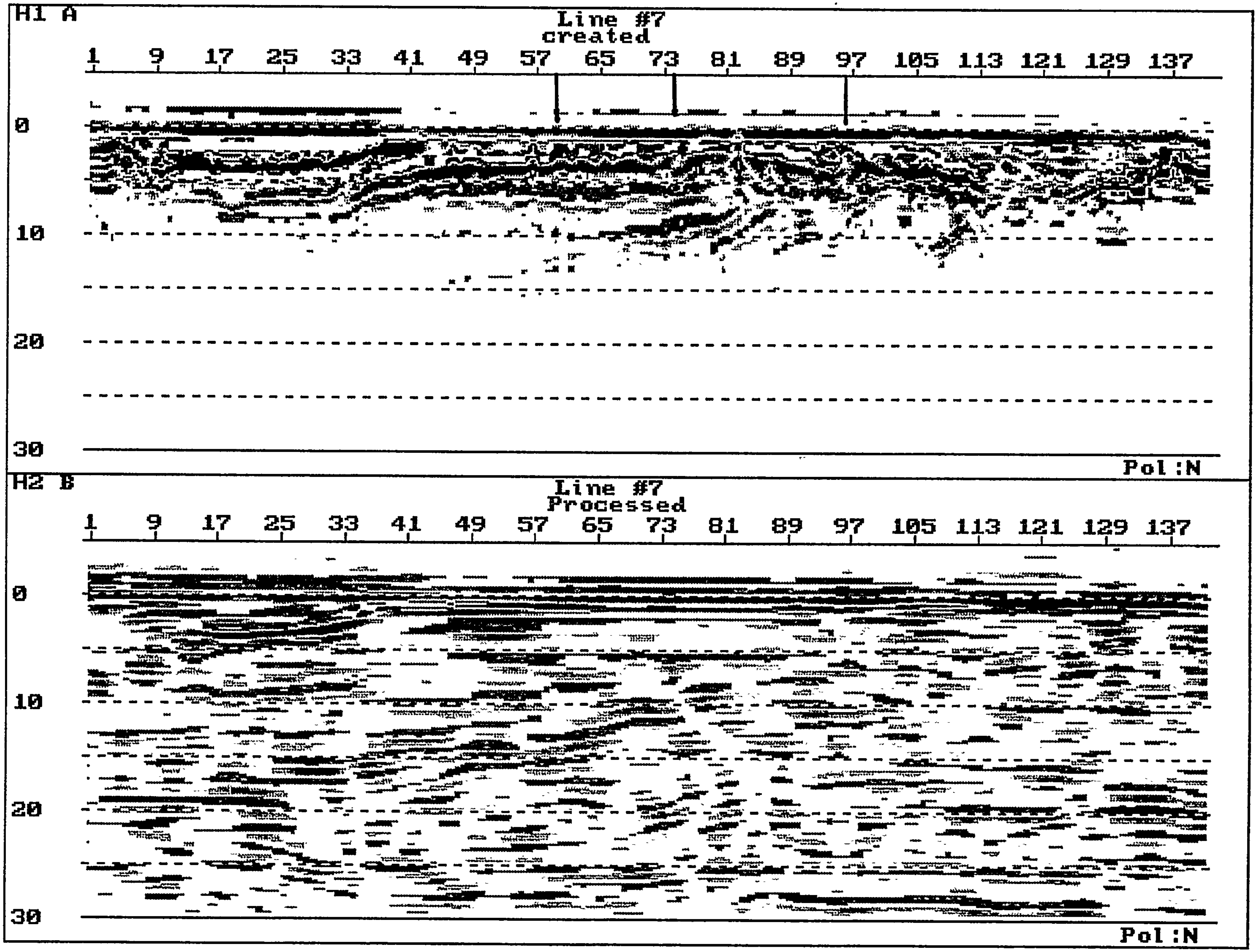
H1 A
Line #7
created
1 9 17 25 33 41 49 57 65 73 81 89 97 105 113 121 129 137
0
10
20
30
Pol :N
H2 B
Line #7
Processed
1 9 17 25 33 41 49 57 65 73 81 89 97 105 113 121 129 137
0
10
20
30
Pol :N

FIGURE 10

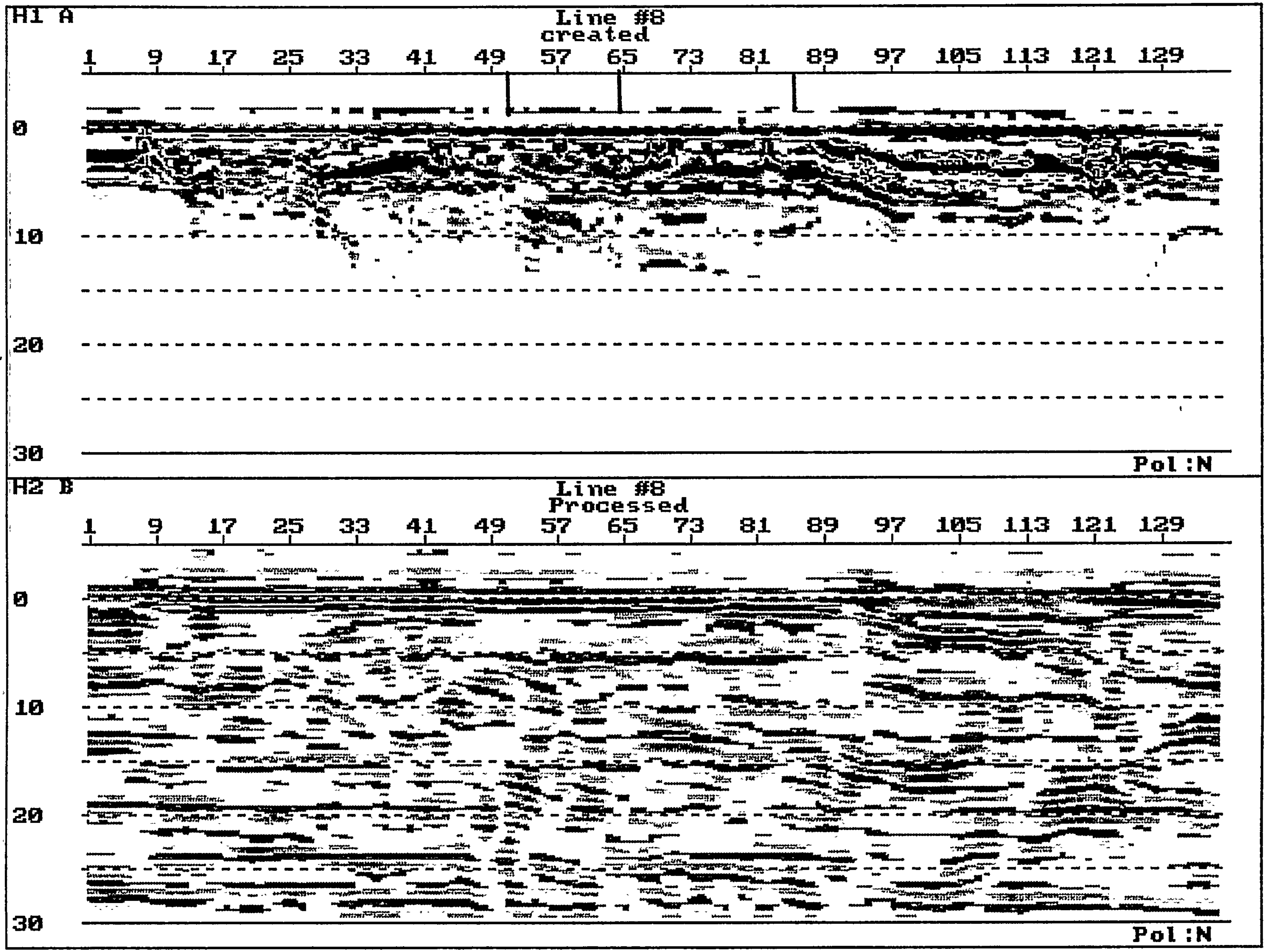
H1 A
Line #8
created
1 9 17 25 33 41 49 57 65 73 81 89 97 105 113 121 129
0
10
20
30
Pol :N
H2 B
Line #8
Processed
1 9 17 25 33 41 49 57 65 73 81 89 97 105 113 121 129
0
10
20
30
Pol :N

FIGURE 11

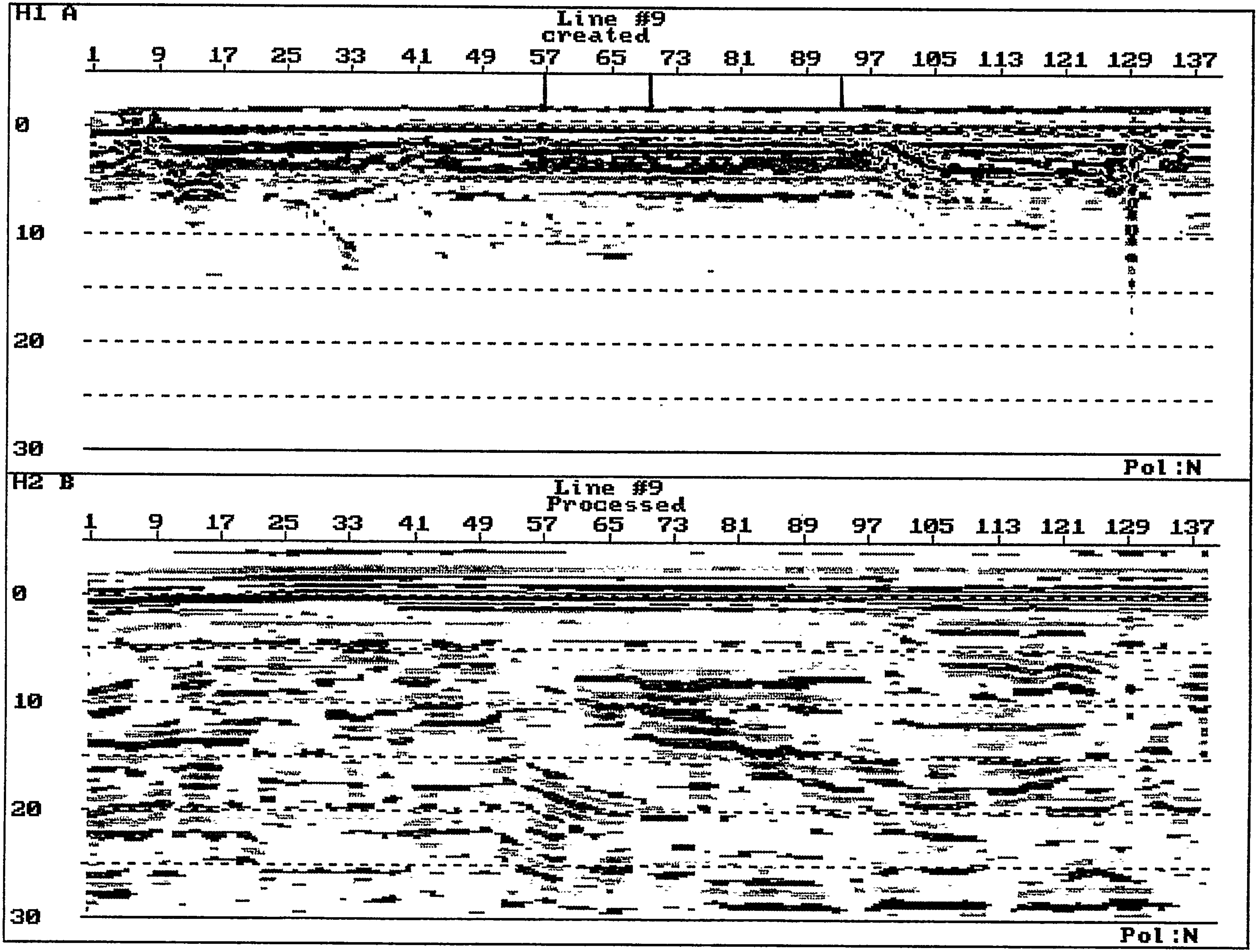
H1 A
Line #9
created
1 9 17 25 33 41 49 57 65 73 81 89 97 105 113 121 129 137
0
10
20
30
Pol:N
H2 B
Line #9
Processed
1 9 17 25 33 41 49 57 65 73 81 89 97 105 113 121 129 137
0
10
20
30
Pol:N

FIGURE 12

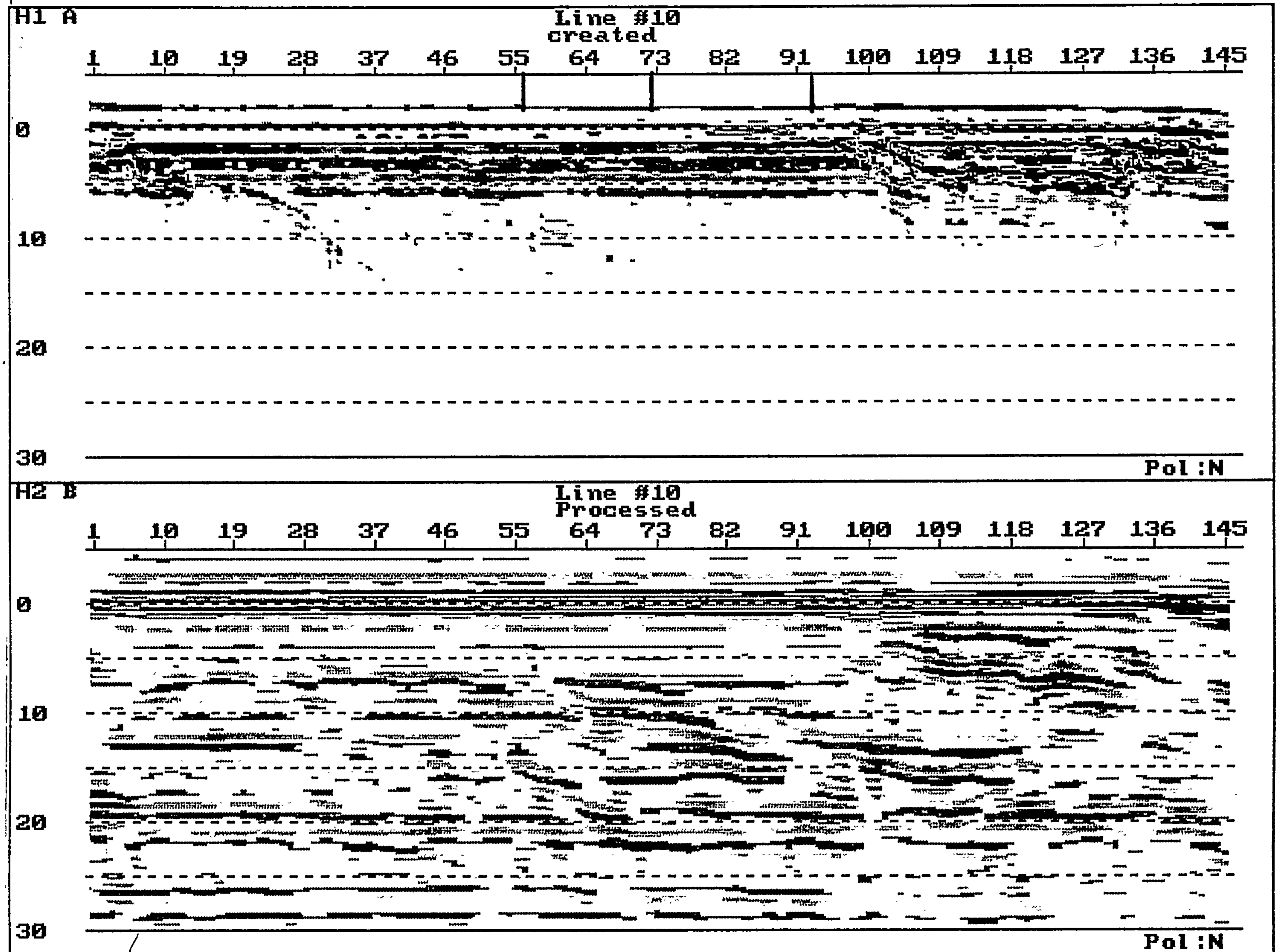
H1 A
Line #10
created
1 10 19 28 37 46 55 64 73 82 91 100 109 118 127 136 145
0
10
20
30
Pol :N
H2 B
Line #10
Processed
1 10 19 28 37 46 55 64 73 82 91 100 109 118 127 136 145
0
10
20
30
Pol :N

FIGURE 13

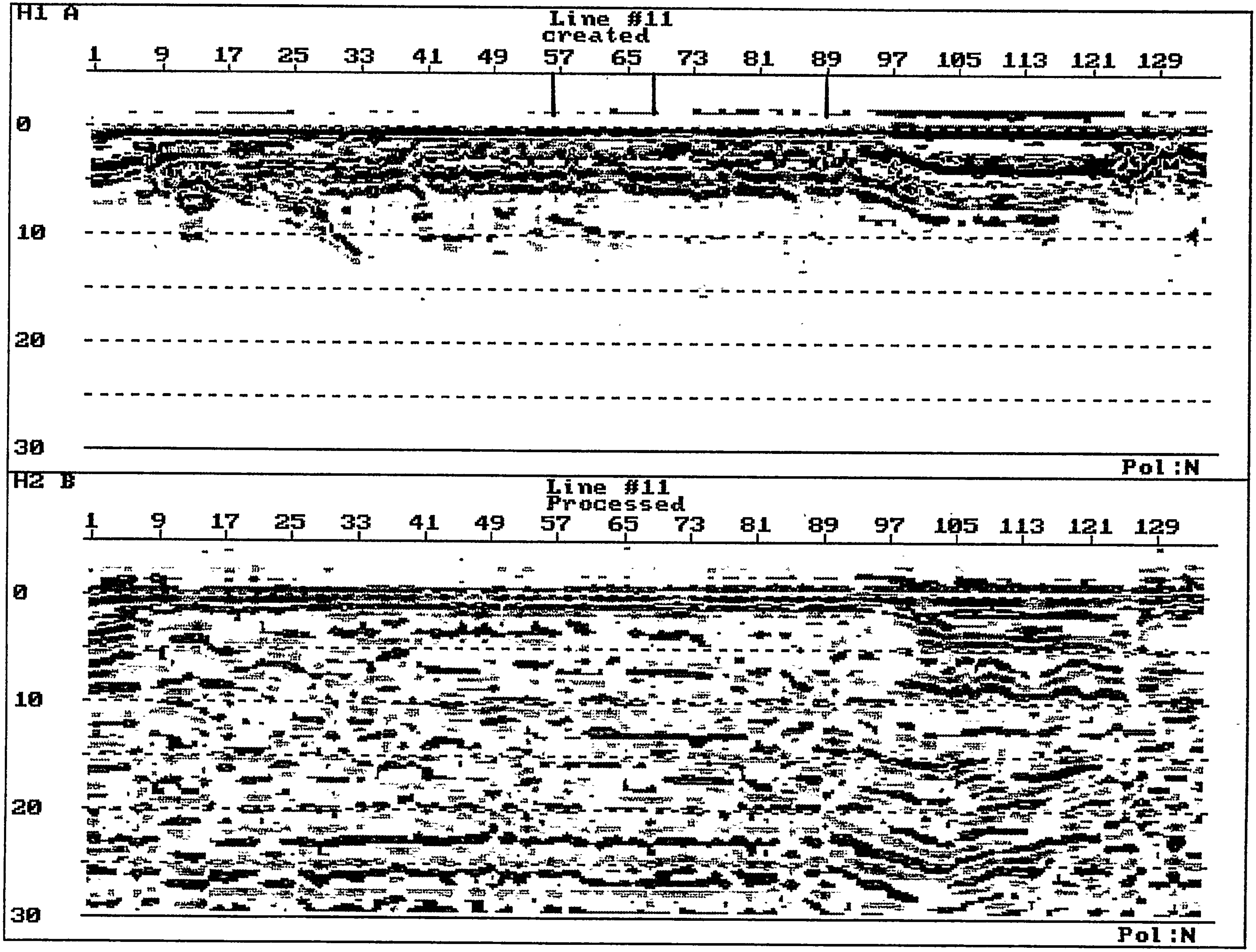
H1 A
Line #11
created
1 9 17 25 33 41 49 57 65 73 81 89 97 105 113 121 129
0
10
20
30
Pol :N
H2 B
Line #11
Processed
1 9 17 25 33 41 49 57 65 73 81 89 97 105 113 121 129
0
10
20
30
Pol :N

FIGURE 14

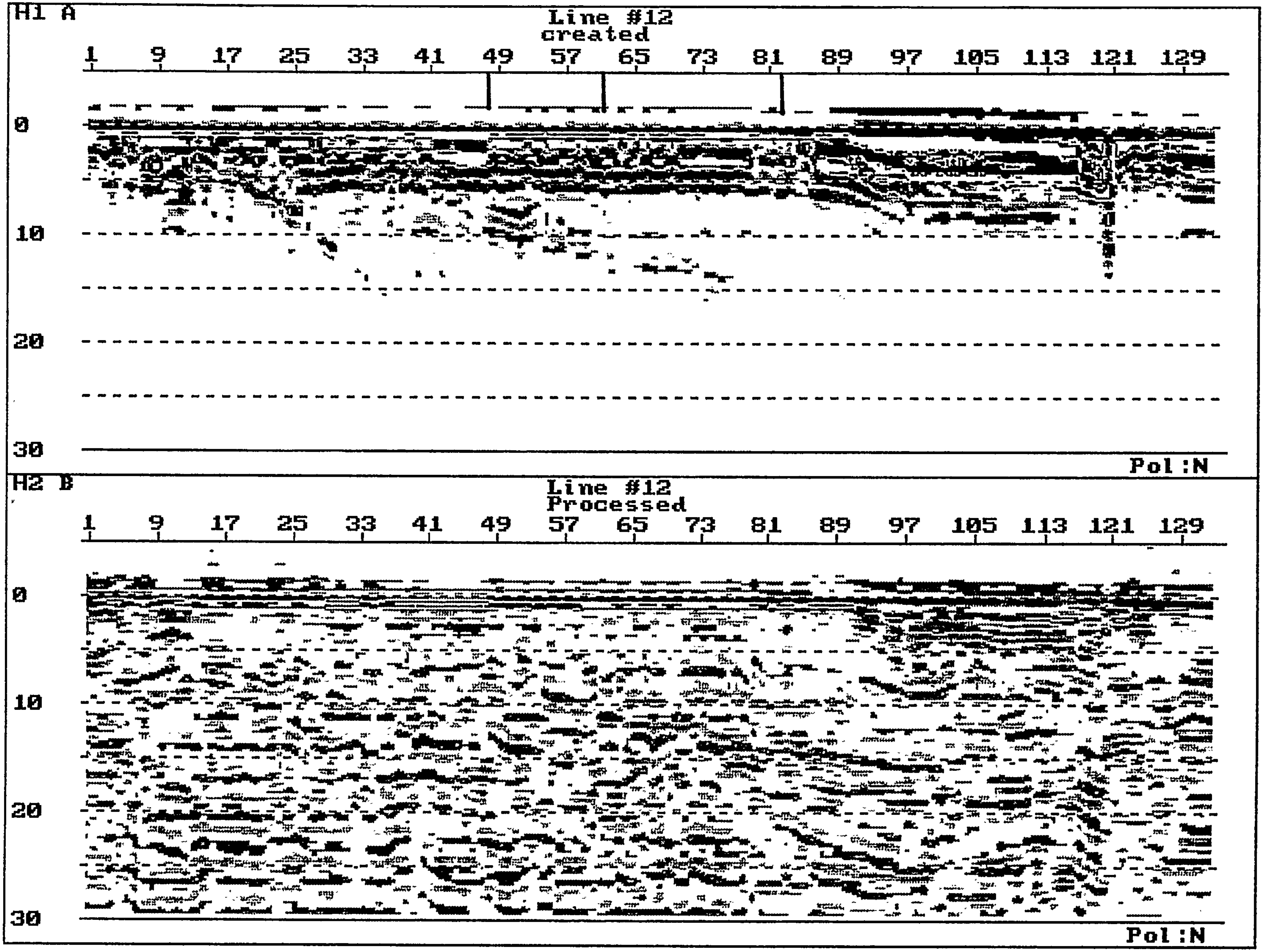
H1 A
Line #12
created
1 9 17 25 33 41 49 57 65 73 81 89 97 105 113 121 129
0
10
20
30
Pol :N
H2 B
Line #12
Processed
1 9 17 25 33 41 49 57 65 73 81 89 97 105 113 121 129
0
10
20
30
Pol :N

FIGURE 15

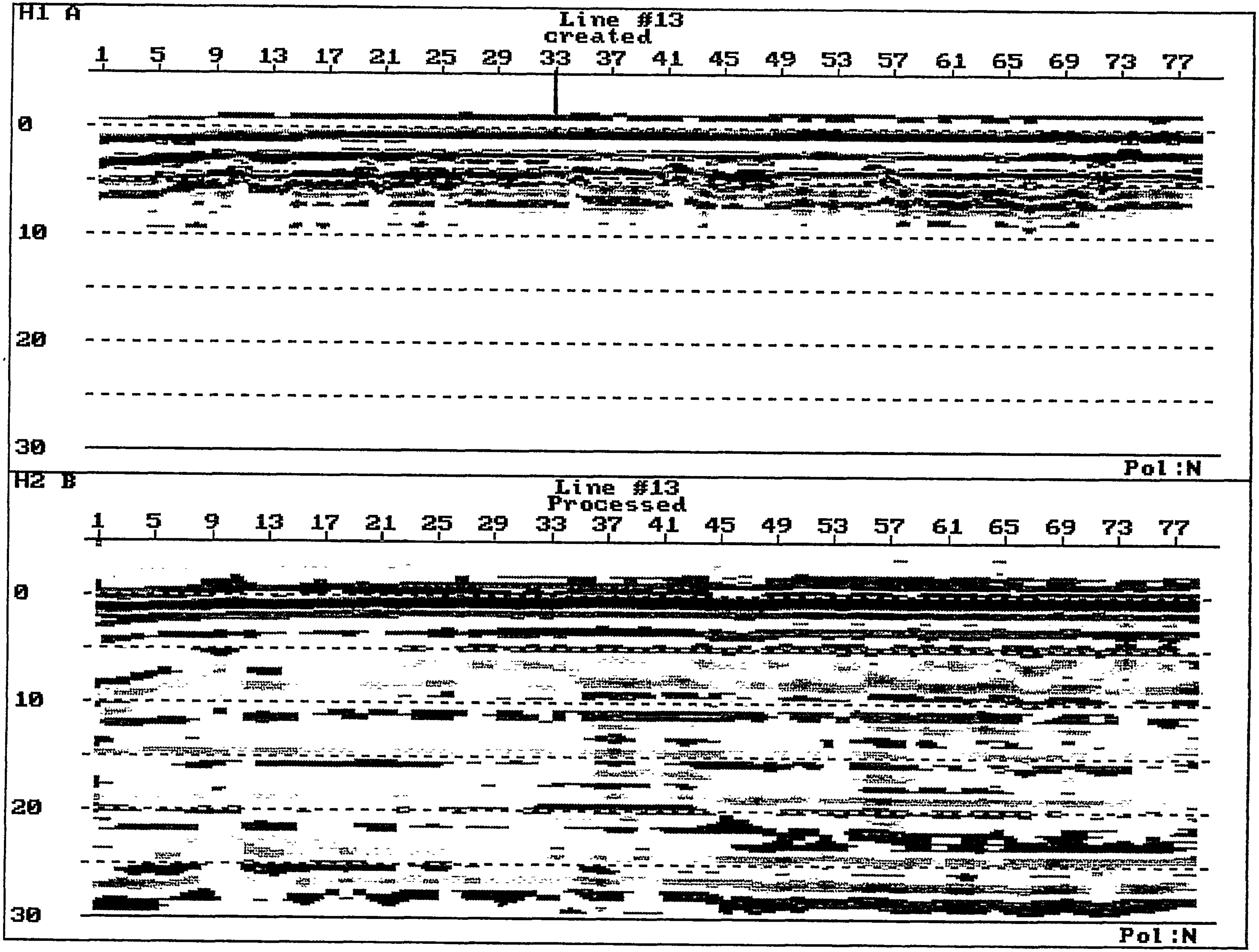
H1 A
Line #13
created
1 5 9 13 17 21 25 29 33 37 41 45 49 53 57 61 65 69 73 77
0
10
20
30
Pol:N
H2 B
Line #13
Processed
1 5 9 13 17 21 25 29 33 37 41 45 49 53 57 61 65 69 73 77
0
10
20
30
Pol:N

FIGURE 16

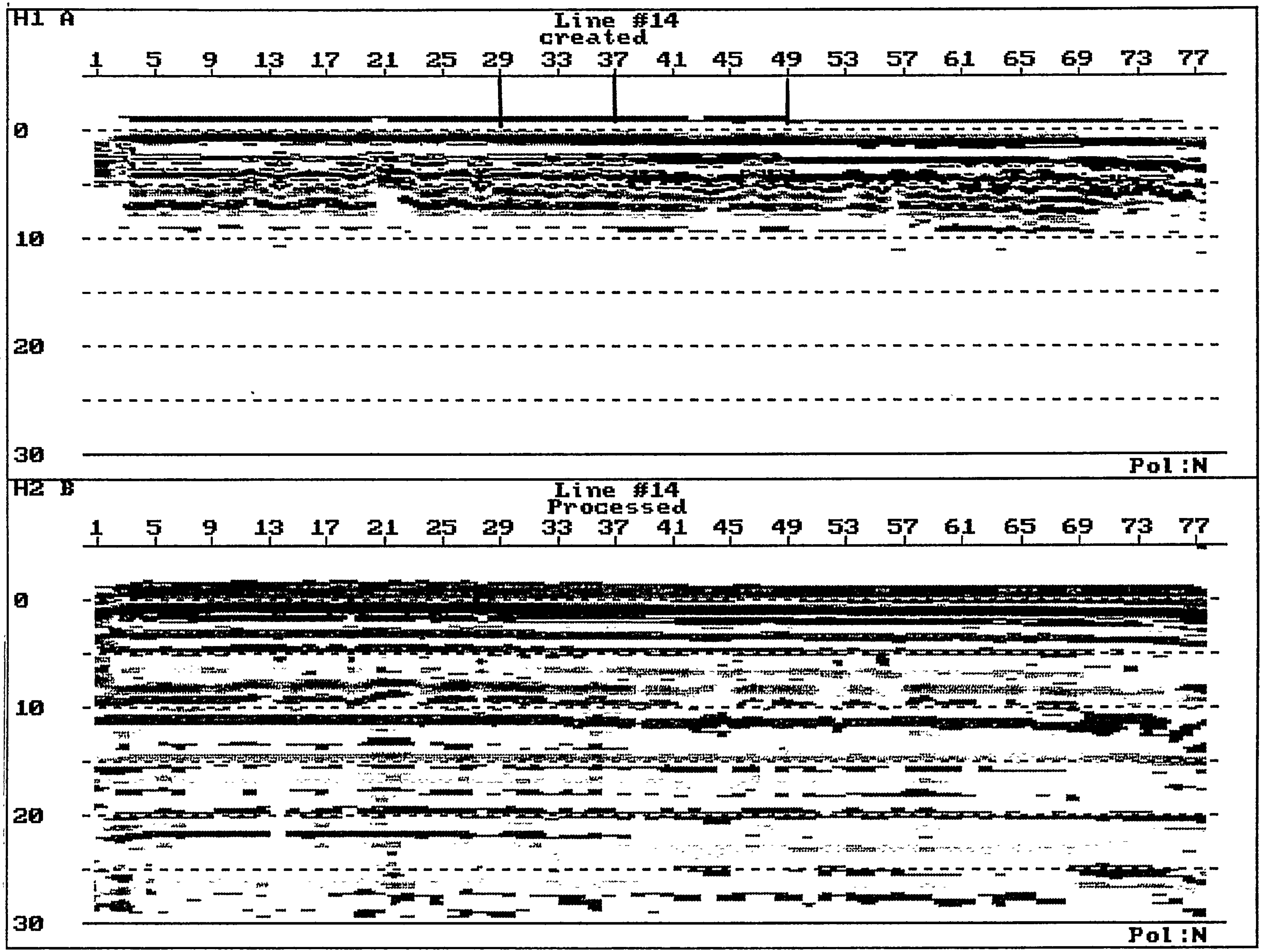
H1 A
Line #14
created
1 5 9 13 17 21 25 29 33 37 41 45 49 53 57 61 65 69 73 77
0
10
20
30
Pol :N
H2 B
Line #14
Processed
1 5 9 13 17 21 25 29 33 37 41 45 49 53 57 61 65 69 73 77
0
10
20
30
Pol :N

FIGURE 17

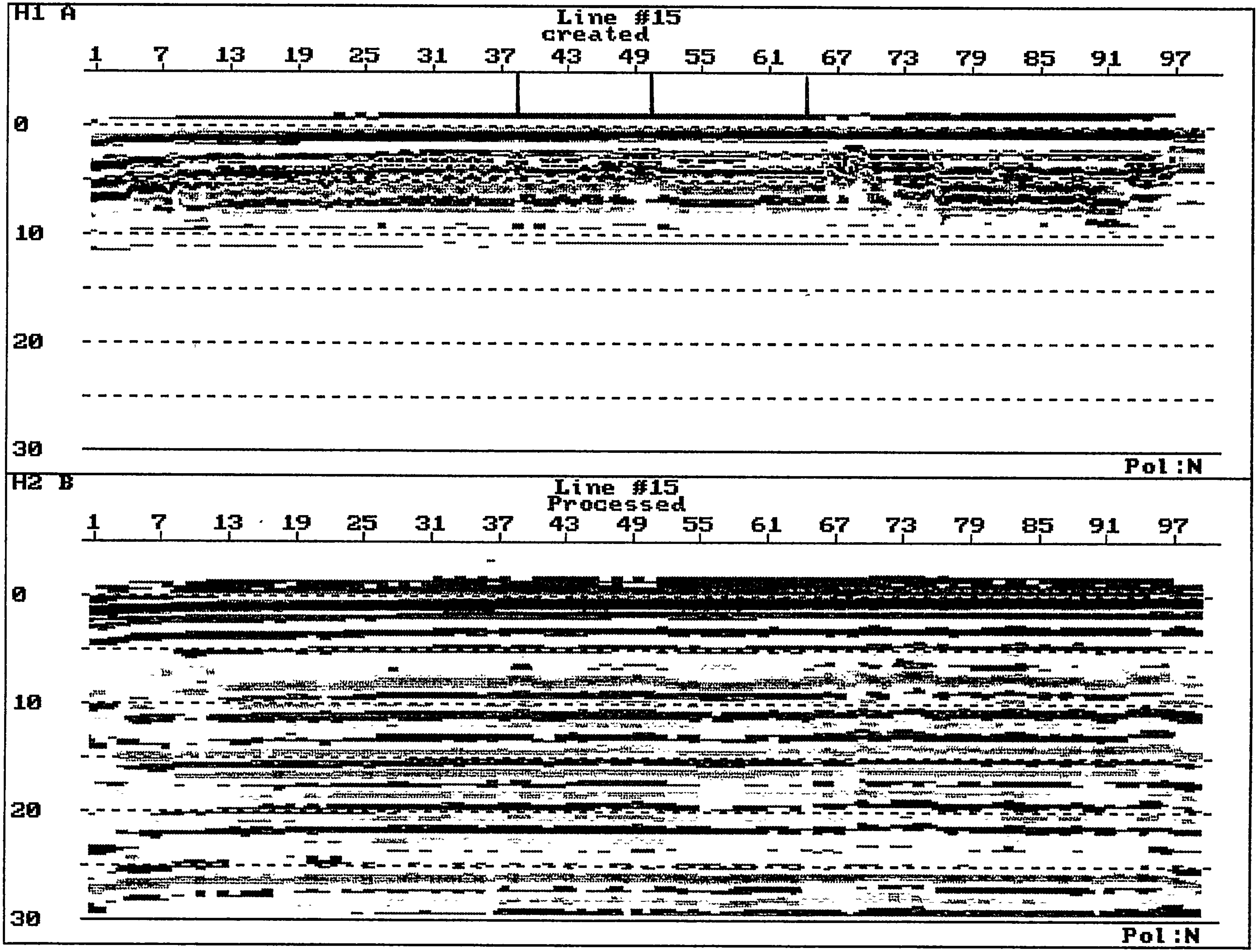
H1 A
Line #15
created
1 7 13 19 25 31 37 43 49 55 61 67 73 79 85 91 97
0
10
20
30
Pol:N
H2 B
Line #15
Processed
1 7 13 19 25 31 37 43 49 55 61 67 73 79 85 91 97
0
10
20
30
Pol:N

FIGURE 18

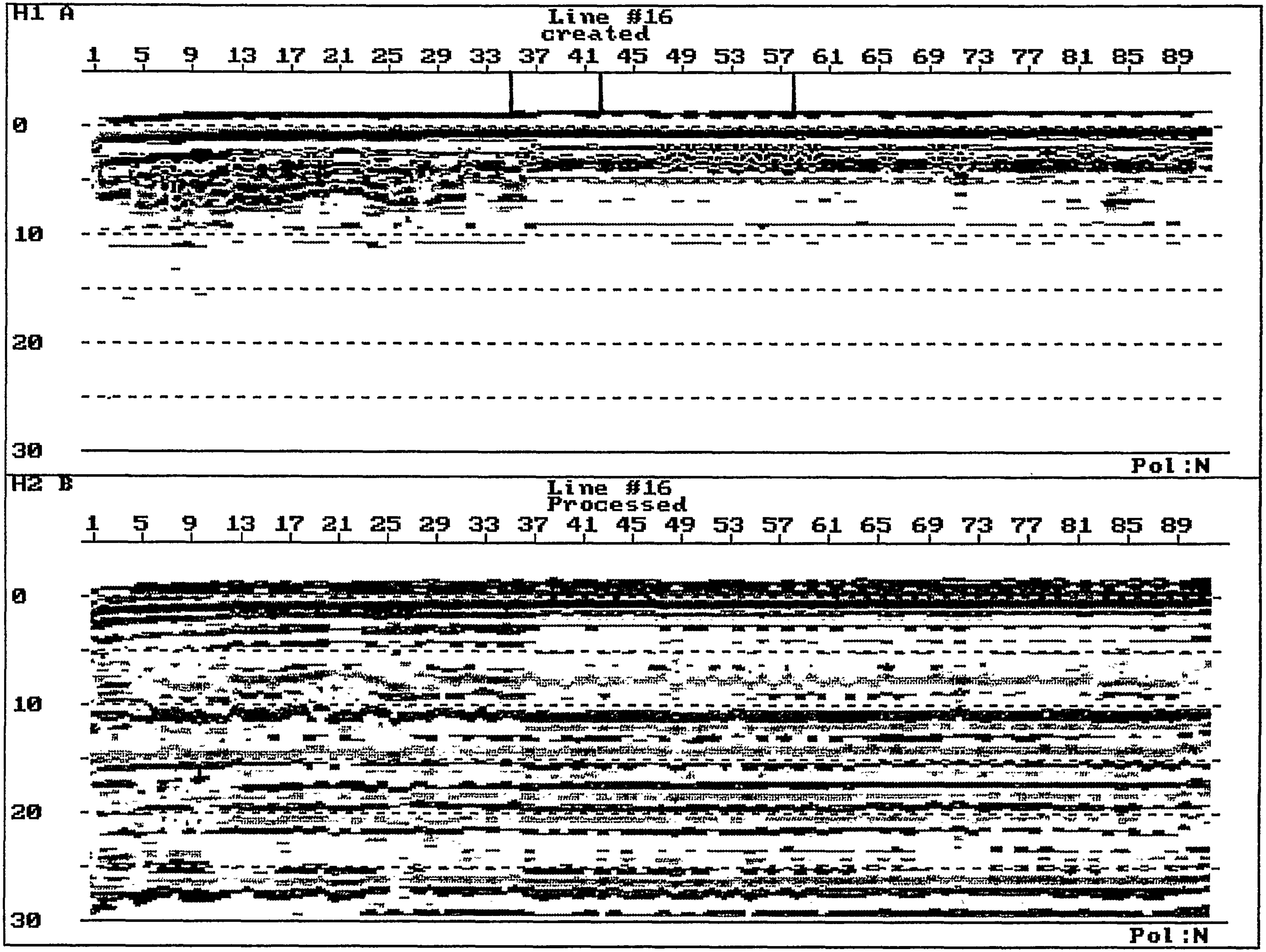
H1 A
Line #16
created
1 5 9 13 17 21 25 29 33 37 41 45 49 53 57 61 65 69 73 77 81 85 89
0
10
20
30
Pol :N
H2 B
Line #16
Processed
1 5 9 13 17 21 25 29 33 37 41 45 49 53 57 61 65 69 73 77 81 85 89
0
10
20
30
Pol :N

FIGURE 19

FIGURE 20

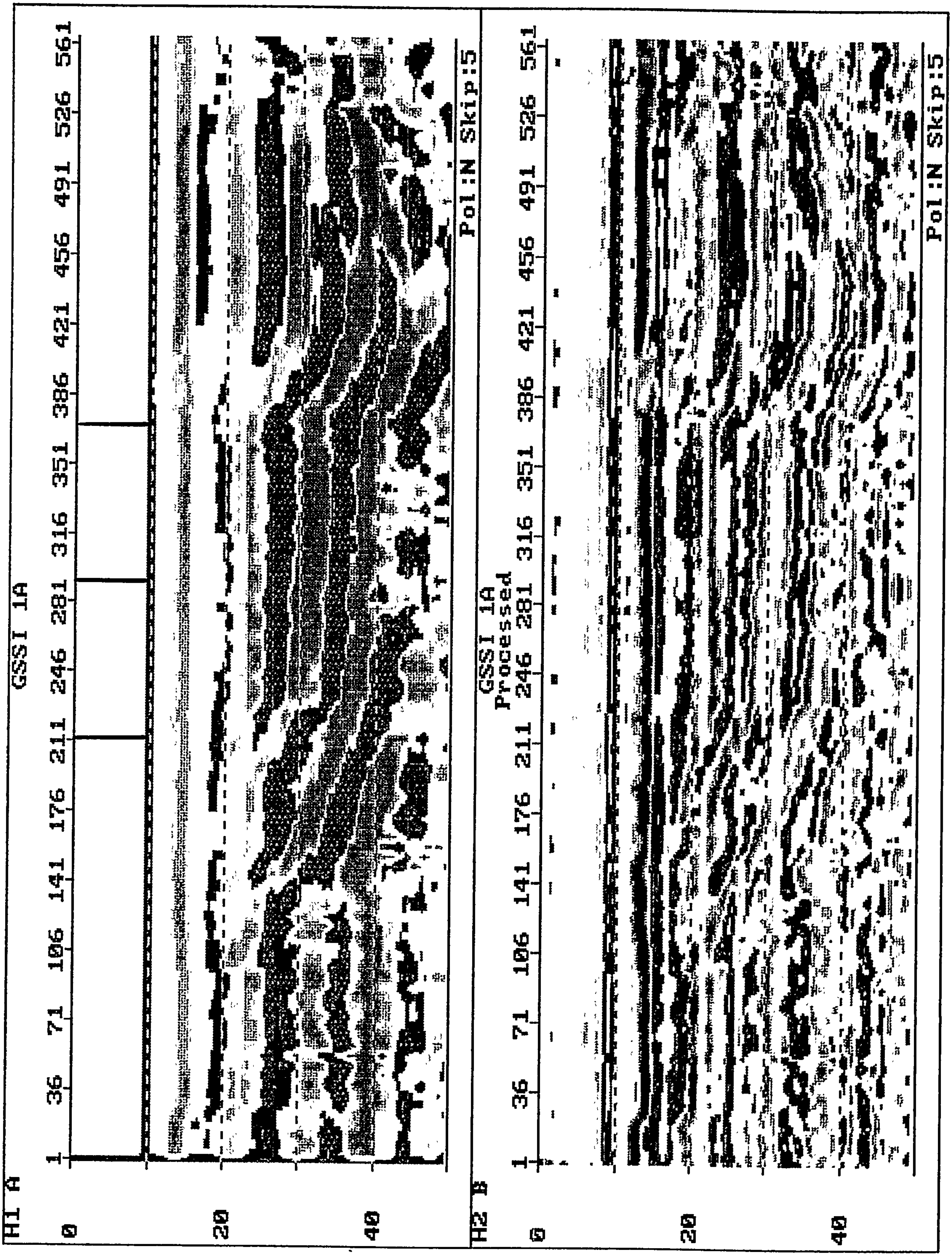
H1 A
GSSI 1A
1 36 71 106 141 176 211 246 281 316 351 386 421 456 491 526 561
0
20
40
Pol:N Skip:5
H2 B
GSSI 1A
Processed
1 36 71 106 141 176 211 246 281 316 351 386 421 456 491 526 561
0
20
40
Pol:N Skip:5

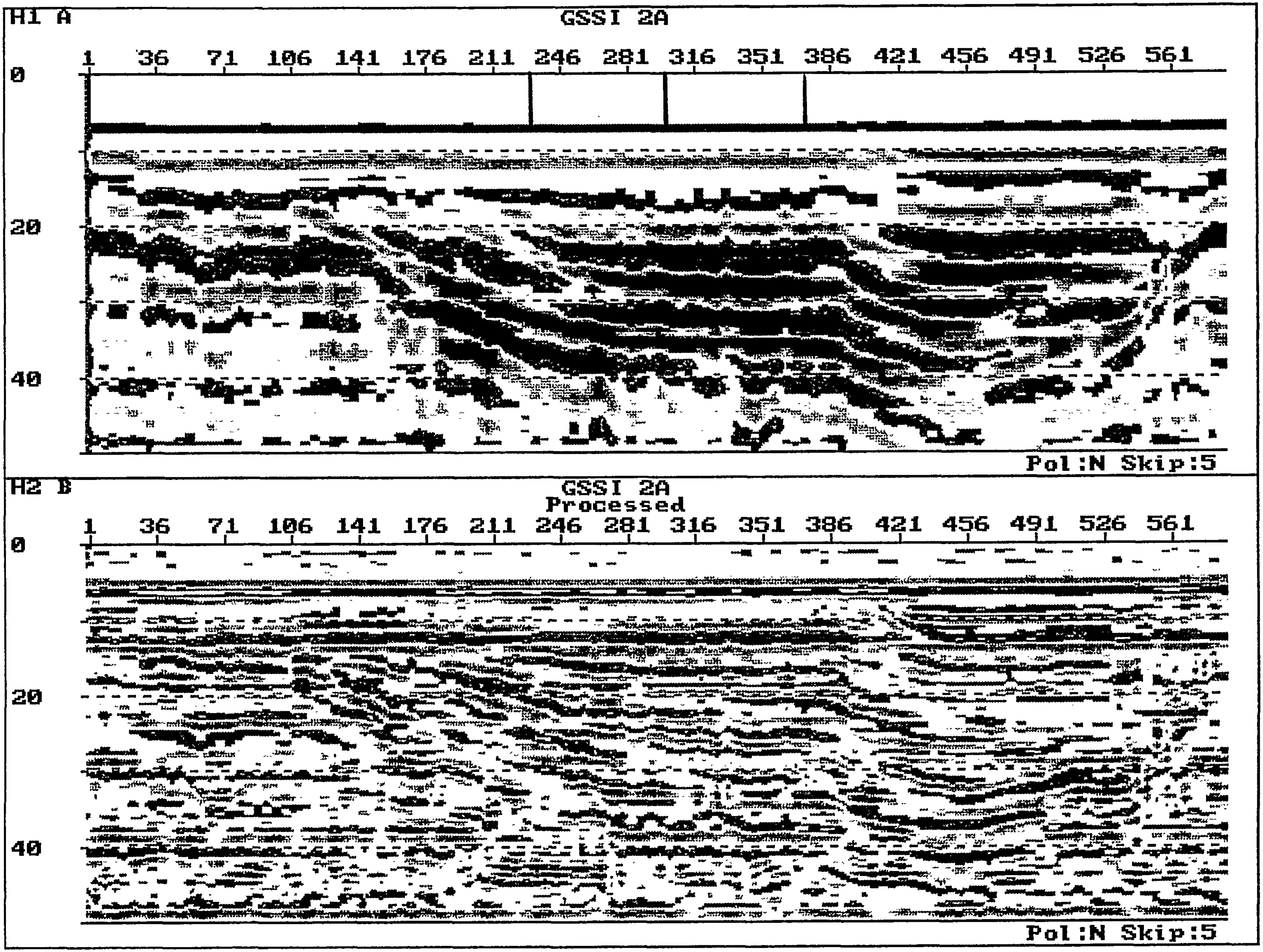
H1 A
GSSI 2A
1 36 71 106 141 176 211 246 281 316 351 386 421 456 491 526 561
0
20
40
Pol:N Skip:5
H2 B
GSSI 2A
Processed
1 36 71 106 141 176 211 246 281 316 351 386 421 456 491 526 561
0
20
40
Pol:N Skip:5

FIGURE 21

MICROSEEPS GPR FIELD LOG

JOB: CLAY TEST Pit DATE: 10-3-95

TERRAIN: WEATHER:

TAPE NUMBER: S&S PE 1000 * FILTERS: L:N: FREQ:

SCANS/FT: VERT. H:N: FREQ:

TICKS/FT: HORIZ. LP: (TC)

RANGE NS: SAMPLES/SCAN:

ANT. MHZ. START NS:

		FILE#	LINE#	FOOTAGE	#SCANS	REMARKS Files 1-4 on GROUND
	1	1	1 ~~61~~	LO-HI		450 MHZ ANT. PULSE Volt = 200
	2		~~62~~			50 NS WINDOW S/R = 300 ps Pts. 166
	3		~~63~~			#STACKS = 32 O/Adj = -25 NS
	4		~~64~~			Ropes @ 103 - 134 - 171 TRACES
	5		~~65~~			START 13' END 161'
	6	2	~~66~~	HI-LO		START 161' END 13'
	7		~~67~~			Ropes @ 92 - 129 - 156 TRACE
	8	3	~~68~~	LO-Hi		SAME AS #1
	9		~~69~~			ROPES 106 - 128 - 171 TRACES
	10	4	~~70~~	HI-LO		SAME AS #2
	11		~~71~~			ROPES 95 - 134 - 159
AIR SHOTS	12	5	~~72~~	LO-Hi		10"-12" ABOVE GRD. OTIME = -10 100NS = WIND
	13		~~73~~			Ropes 42 - 52 - 67 TRACES
	14	6	~~74~~	HI-LO		10"-12" ABOVE GRD.
	15		~~75~~			ROPES ? - 46 - 56 TRACES
	16	7	~~76~~	LO-HI		100 NS-WIND O = -20 NS 1000 GAIN
	17		~~77~~			ROPES 60 - 74 - 96 TRACES
	18	8	~~78~~	HI-LO		SAME AS #7 300 GAIN
	19		~~79~~			ROPES 57 - 72 - 85
	20		80			END @ TRACE 132

PAGE 1 OF 2

MICROSEEPS GPR FIELD LOG

JOB: CLAY TEST PIT | DATE: 10-3-95

TERRAIN: | WEATHER:

TAPE NUMBER: | FILTERS: L:N: FREQ:

SCANS/FT: | VERT. H:N: FREQ:

TICKS/FT: | HORIZ. LP: (TC)

RANGE NS: | SAMPLES/SCAN:

ANT. MHZ. | START NS:

		FILE#	LINE#	FOOTAGE	#SCANS	REMARKS
	1	9	~~81~~	LO-HI		GAIN 600 ANT - 2" off GRD. RANGE 100
AIR Shots	2		~~82~~			ROPES @ 56 - 70 - 92 TRACES
	3	10	~~83~~	HI-LO		SAME AS #9 - 2" OFF GRD
	4		~~84~~			ROPES @ 54 - 74 - 90 TRACES
	5	11	~~85~~	LO-HI		ON GRD GAIN 600 NEW ANT - ORIEN.
	6		~~86~~			ROPES @ 56 - 68 - 89
	7	12	~~87~~	HI-LO		GAIN 200 NEW ANT. ORIEN
	8		~~88~~			ROPES @ 51 - 72 - 85
	9	13	~~89~~	LO-HI		12" IN AIR START -10 NS NEW ANT. ORIEN
AIR Shots	10		~~90~~			ROPES @ 33 - ? - ?
	11	14	~~91~~	HI-LO		12" IN AIR
	12		~~92~~			ROPES @ 29 - 41 - 49
	13	15	~~93~~	LO-HI		12" IN AIR NEW ANT ORIEN
AIR Shots	14		~~94~~			ROPES @ 39 - 50 - 64
	15	16	~~95~~	HI-LO		12" IN AIR
	16		~~96~~			ROPES @ 34 - 50 - 57
	17		~~97~~	GSSI RADAR SYS		
	18	1	~~98~~	LO-HI		2 FILES 300 MHZ
	19	2	~~99~~	HI-LO		2 FILES 300 MHZ
	20		~~100~~			SIR10 - 100395 1729 TAPE

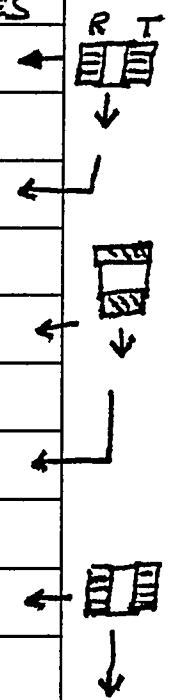

PAGE 2 OF 2

PROFILE

Clay test Pit
10-3-95